Reconfiguration of square-tiled surfaces

Vincent Delecroix[1] and Clément Legrand-Duchesne[1,2]

[1] *CNRS, LaBRI, Université de Bordeaux, Bordeaux, France.*
[2] *Theoretical Computer Science Department, Faculty of Mathematics and Computer Science, Jagiellonian University, Kraków, Poland.*

January 27, 2025

Abstract

We consider a combinatorial reconfiguration problem on a subclass of quadrangulations of surfaces called square-tiled surfaces. Our elementary move is a shear in a cylinder that corresponds to a well-chosen sequence of diagonal flips that preserves the square-tiled properties. We conjecture that the connected components of this reconfiguration problem are in bijection with the connected components of the moduli space of quadratic differentials. We prove that the conjecture holds in the so-called hyperelliptic components of Abelian square-tiled surfaces. More precisely, we show that any two such square-tiled surfaces of genus g can be connected by $O(g)$ powers of cylinder shears.

1 Introduction

In this article, we consider the combinatorial reconfiguration problem given by the action of cylinder shears on the set of square-tiled surfaces. We review in Subsection 1.1 combinatorial reconfiguration that aims to study reachability or connectivity of state spaces from either a geometric or computational perspective. We next turn in Subsection 1.2 to a classical combinatorial reconfiguration of geometric origin: diagonal flips in graphs embedded in surfaces. The latter is relevant as a square-tiled surface is a special case of quadrangulation and a cylinder shear can be decomposed as a sequence of diagonal flips. In Subsection 1.3, we define cylinder shears on square-tiled surfaces and state a conjectural classification of connected components for cylinder shears on square-tiled surfaces (Conjecture 1.4). We then state our main result which settles some special cases of this conjecture (Theorem 1.6).

1.1 Combinatorial reconfiguration

Combinatorial reconfiguration aims to study the action of the monoid generated by a set of (possibly partial) functions $\{f_i : X \to X\}$, called the *(combinatorial) moves* on some finite set X called the *state space*. This situation can conveniently be encoded in the *reconfiguration graph* (which is an oriented multi-graph) whose set of vertices is X and whose set of edges is $\{(x, f_i(x)) : x \in X, i \in I\}$. Most often, X is a "complicated" set and the moves are "elementary" in the sense that x does not "differ" much from $f_i(x)$.

Famous reconfiguration problems include games such as the Rubik's Cube or Sokoban for example, or problems on graphs such as reconfiguration of independent sets or colourings (see the comprehensive surveys [vdH13, Nis18, MN19]).

One crucial question in combinatorial reconfiguration is the connectedness of the reconfiguration graph (equivalently the transitivity of the action). More precisely, one would like to find simple invariants or efficient procedures to decide if two elements of the state space are equivalent, that is, belong to the same connected component. A natural refinement of this question consists in studying the geometry of the connected components, e.g. their diameter.

When the combinatorial moves are endowed with probabilities, this turns the action into a Markov chain (see [LP17] for an introduction to Markov chains and their analysis). Under favourable conditions, the chain is irreducible if the action is transitive and its stationary measure is the uniform measure on X. A necessary condition for this to happen is the connectedness of the reconfiguration graph. In such case, a simulation of the Markov chain gives access to a random generator of elements in X. This goes under the name of *Monte-Carlo* generator. The quality of this generator which is generally not uniform after a finite execution of the Markov chain is quantified by the so-called mixing time. This random generation turns out to be one important motivation for combinatorial reconfiguration both from a theoretical and an experimental perspective.

1.2 Edge flip in polygons and embedded graphs

Consider a convex n-gon and its triangulations. The *flip* operation consists in flipping an edge: remove an edge of the triangulation and replace it with the other diagonal in the created quadrilateral. In that context, the reconfiguration graph $\mathcal{T}_n$ is usually called a *flip graph*. Sleator, Tarjan and Thurston [STT88], completed by the work of Pournin [Pou14], proved that the diameter of the flip graph $\mathcal{T}_n$ is equal to $2n-10$ for $n \geqslant 13$. This is one of the very few examples where the value of the diameter of the reconfiguration graph is exactly known. Molloy, Reed and Steige [MRS99] proved that the associated Markov chain, called the *flip dynamics*, mixes rapidly. Since then, the mixing time of the flip dynamics has been improved several times, although the exact rate is not known and has been conjectured by Aldous [Ald94] to be $O(n^{3/2})$, up to logarithmic factors. The current best upper bound of $O(n^3 \log^3(n))$ is due to Eppstein and Frishbreg [EF23].

Let us now move from polygons to graphs embedded in surfaces. Let e be an edge adjacent to two distinct faces of degree d_1 and d_2 in an embedded graph. A *flip* of e consists in first removing e from the graph (see Figure 1). This merges the two adjacent faces into one of degree $d_1 + d_2 - 2$. Then, we reintroduce an edge e' inside the newly created face. Note that among the flips associated to e there are some that preserve the faces' degrees.

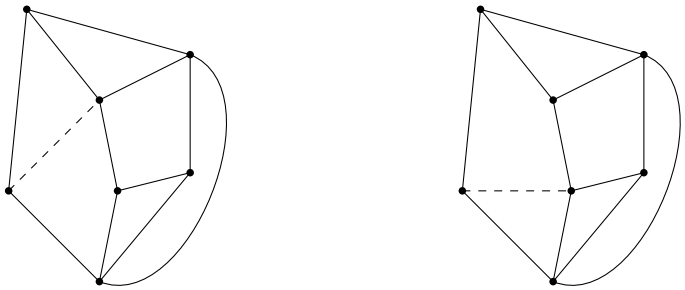

Figure 1: Two combinatorial maps that differ by one flip. The flipped edge is dashed. This flip preserves the degree of the faces.

Let $\mathcal{T}_{g,n}$ and $\mathcal{Q}_{g,n}$ be respectively the set of isomorphism classes of triangulations and of quadrangulations of genus g with n vertices. One can turn $\mathcal{T}_{g,n}$ and $\mathcal{Q}_{g,n}$ into reconfiguration

graphs by putting an edge between m and m' if m and m' are related by a flip. The connectedness of $\mathcal{T}_{g,n}$ has been proved by various geometric and combinatorial methods, see [Mos88] and the references therein. Estimates on the diameter have only been settled recently in the most general situation.

Theorem 1.1 (Disarlo-Parlier [DP19]). *The diameter of $\mathcal{T}_{g,n}$ is $\Theta(g\log(g+1)+n)$.*

Let us mention that the lower bound on the diameter follows from the techniques in [STT92]. The case of the sphere ($g=0$) has received more attention and more precise asymptotics are known, see [Pou14, Fra17, PP17, CHK+18, PP18a, PP18b].

Finally, we consider some results concerning the mixing time in the case of the sphere. We denote $\mathcal{T}_{g,n}^{root}$ and $\mathcal{Q}_{g,n}^{root}$ the triangulations and quadrangulations of genus g with n vertices and one rooted edge, that is distinguished and oriented[1].

Theorem 1.2 ([Bud17, CS20]). *The flip dynamics on $\mathcal{T}_{0,n}^{root}$ has mixing time $\Omega(n^{5/4})$. The flip dynamics on $\mathcal{Q}_{0,n}^{root}$ has mixing time $\Omega(n^{5/4})$ and $O(n^{13/2})$.*

1.3 Cylinder shear in square-tiled surfaces

A square-tiled surface is a quadrangulation of a connected surface with a 2-colouring of its edges such that all faces have an alternating boundary. One obtains a square-tiled surface geometrically by taking copies of a unit square and gluing horizontal edges to horizontal edges and vertical edges to vertical edges. We refer the reader to Subsection 2.1 for more detailed definitions. Square-tiled surfaces were introduced in the context of Abelian and quadratic differentials on Riemann surfaces by Zorich [Zor02]. In this article, we will actually consider a slight generalization of square-tiled surfaces where we allow *folded edges* which turns out to be crucial in our connectedness proof (see Subsection 2.1 for a precise definition).

In general, a single diagonal flip operation does not preserve the square-tiled property of the surface. Indeed, diagonal flips change the parity of the degree of the vertices incident to the flipped edge (see Figure 2), but the 2-colouring of the edges of the square-tiled surfaces imposes the vertices to have even degrees.

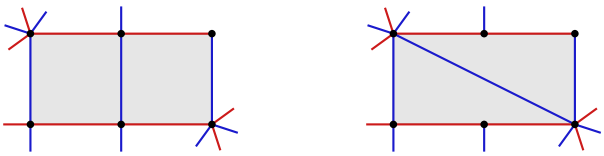

Figure 2: Diagonal flips do not preserve square-tiled surfaces.

A *horizontal cylinder* in a square-tiled surface is a cycle of squares adjacent along their vertical edges. A *horizontal cylinder shear* consists in doing all flips on the vertical edges in the cylinder (see Figure 3). Note that these flips commute. One defines similarly *vertical cylinders* and their shears. Cylinder shears hence preserve the set of square-tiled surfaces and the number of squares. We will see in Subsection 2.2, that cylinder shears present unexpected similarities with another reconfiguration operation: Kempe changes on graph colourings.

Beyond the number of squares, it turns out that the degree of the vertices is also invariant under cylinder shears. The *profile* of a square-tiled surface is a pair (μ, k) made of an integer

[1]Note that our definitions of $\mathcal{T}_{g,n}^{root}$ and $\mathcal{Q}_{g,n}^{root}$ differ from [CS20, Bud17], in which n denotes the number of faces. However, by Euler's formula, the number of faces is proportional to the number of vertices, up to an additive term which is linear in the genus. Hence, their results extend to our definitions of $\mathcal{T}_{g,n}^{root}$ and $\mathcal{Q}_{g,n}^{root}$.

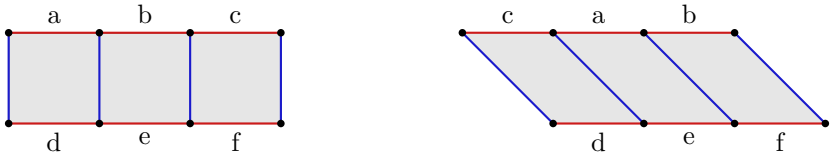

Figure 3: A horizontal cylinder shear.

partition $\mu = [1^{\mu_1}, 2^{\mu_2}, \ldots]$ where μ_i is the number of vertices of degree $2\mu_i$ and k is the number of folded edges. Euler's formula relates the profile (μ, k) to the genus g of the underlying surface as follows,

$$\sum_{i \geqslant 1} \mu_i (i-2) = 4g - 4 + k. \tag{1}$$

We let $\mathrm{ST}(\mu, k)$ denote the set of square-tiled surfaces with given profile (μ, k) and by abuse of notation $\mathrm{ST}(\mu)$ when $k = 0$.

It turns out that $\mathrm{ST}(\mu, k)$ might still be non-connected under cylinder shears. We introduce a first invariant of the connected components. Let τ be a square-tiled surface. We say that τ is *Abelian* if one can build this surface in such way that the top sides are only glued to the bottom sides, and the right sides to the left sides. We say that τ is *quadratic* otherwise. Let $\mathrm{ST}_{Ab}(\mu, k)$ and $\mathrm{ST}_{quad}(\mu, k)$ be respectively the set of Abelian and quadratic square-tiled surfaces in $\mathrm{ST}(\mu, k)$. In Figure 4 we show an Abelian and a quadratic square-tiled surface in the stratum $\mathrm{ST}([4^2], 0)$. It is easy to see that the profile (μ, k) of an Abelian square-tiled surface is such that $k = 0$ and the entries in μ are even, that is $\mu_{2i+1} = 0$ for all $i \geqslant 0$.

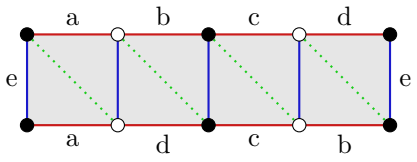

(a) An Abelian square-tiled surface in $\mathrm{ST}_{Ab}([4^2])$ (stratum $\mathcal{H}(1^2)$).

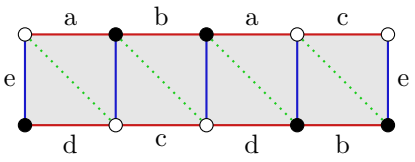

(b) A quadratic square-tiled surface in $\mathrm{ST}_{quad}([4^2])$ (stratum $\mathcal{Q}([2^2])$).

Figure 4: Two square-tiled surfaces in $\mathrm{ST}([4^2])$ (genus $g = 2$) that are not connected under cylinder shears.

The names Abelian and quadratic are borrowed from the theory of Riemann surfaces and their Abelian and quadratic differentials. It turns out that our main conjecture for the connectedness under cylinder shears (Conjecture 1.4 below) is intimately linked to them. We introduce the necessary background now and refer the reader to Section 2 for more details. To each square-tiled surface, one can associate a Riemann surface endowed with a quadratic differential. It turns out that $\mathrm{ST}_{Ab}(\mu)$ (respectively $\mathrm{ST}_{quad}(\mu, k)$) corresponds to the quadratic differentials that are the squares of an Abelian differential (resp. not the square of an Abelian differential). The moduli space of the Abelian differentials and the quadratic differentials that are not the square of an Abelian one are stratified according to the degree of their zeros. The stratum of the Abelian differentials associated to the square-tiled surfaces in $\mathrm{ST}_{Ab}(\mu)$ is denoted $\mathcal{H}(1^{\kappa_1}, 2^{\kappa_6}, \ldots)$, where $\kappa_i = \mu_{2i+2}$, while the one associated to $\mathrm{ST}_{quad}(\mu, k)$ is denoted $\mathcal{Q}(-1^{\kappa_{-1}}, 1^{\kappa_1}, 2^{\kappa_2} \ldots)$, where $\kappa_{-1} = \mu_1 + k$ and for $i \geqslant 1, \kappa_i = \mu_{i+2}$. Let us emphasise that μ_2 does not play any role in the associated stratum. The strata are not necessarily connected but their connected components have been classified by Kontsevich and Zorich [KZ03] and by Lanneau [Lan08]. As a consequence of this classification we have that:

Theorem 1.3 ([KZ03, Lan08]).

1. *Each Abelian stratum $\mathcal{H}(\kappa)$ has at most three connected components.*
2. *Each quadratic stratum $\mathcal{Q}(\kappa)$ has at most two connected components.*
3. *In genus 0, that is $\sum_{i\geqslant -1} i\cdot\kappa_i = -4$, $\mathcal{Q}(\kappa)$ is non-empty and connected.*

In this article we will focus on the genus 0 case and some specific connected components of $\mathcal{H}(\kappa)$ in higher genera that are called *hyperelliptic components* (see Section 2 for the definition). For now, let us just mention that for $\mu=[2^{\mu_2},4g-2]$ or $\mu=[2^{\mu_2},(2g)^2]$ where $g\geqslant 2$ and $\mu_2\geqslant 0$, there is a subset $\mathrm{ST}^{hyp}_{Ab}(\mu)$ of $\mathrm{ST}_{Ab}(\mu)$, closed under cylinder shears, which corresponds to the hyperelliptic connected component of $\mathcal{H}(2g-2)$ or $\mathcal{H}((g-1)^2)$ respectively.

We conjecture that the connected components of the moduli space partition the square-tiled surfaces into equivalence classes for the shearing operation:

Conjecture 1.4 (Generalizing Conjecture 4 in [BLdM+22]). *Let μ be an integer partition of n and k a non-negative integer such that*

$$\sum_{i\geqslant 1}\mu_i(i-2)=4g-4+k.$$

Let S and S' be two square-tiled surfaces in $\mathrm{ST}(\mu,k)$. Then S and S' are equivalent via cylinder shears if and only if they belong to the same connected component of the moduli space of quadratic differentials.

According to Theorem 1.3, each $\mathrm{ST}(\mu,k)$ would then be made of at most 5 connected components under cylinder shears. Conjecture 1.4 is a direct generalization of Conjecture 4 in [BLdM+22], which was supported by numerical evidence, to square-tiled surfaces with folded edges.

It is relatively straightforward to prove that being in the same connected component of the moduli space is a necessary condition:

Proposition 1.5. *Let S be a square-tiled surface and S' obtained from S by a cylinder shear. Then the quadratic differentials associated to S and S' belong to the same connected component of the strata of the moduli space of quadratic differentials.*

The underlying reason of Proposition 1.5 is that a cylinder shear can be realised in the moduli space as a continuous motion. Our main contribution is the two following theorems that provide a partial answer to Conjecture 1.4.

Theorem 1.6. *Let $g\geqslant 1$ and $\mu=[2^{\mu_2},4g-2]$ or $\mu=[2^{\mu_2},(2g)^2]$. Then any two square-tiled surfaces in $\mathrm{ST}^{hyp}_{Ab}(\mu)$ are connected by a sequence of at most $\Theta(g)$ powers of cylinder shears.*

Theorem 1.7. *Let μ be an integer partition and k a positive integer such that $\sum\mu_i(i-2)=k-4$. Then $\mathrm{ST}(\mu,k)$ is non-empty. Moreover, if $\mu_1\leqslant 1$, then $ST(\mu,k)$ is connected and has diameter $\Theta(k)$ with respect to powers of cylinder shears.*

Theorem 1.7 generalises a result of Cassaigne, Ferenczi and Zamboni [CFZ11] that proves the case of $\mathrm{ST}([k-2],k)$. Some natural extensions of our results would be to prove Conjecture 1.4 for the quadratic hyperelliptic components or for generic profiles (μ,k) in genus 0, that is without restrictions on μ_1.

As we already mentioned, the connectedness of $\mathrm{ST}([k-2],k)$ under cylinder shears was considered in [CFZ11]. One of their motivation was the theory of dynamical systems and more precisely, the dynamics of interval exchange transformations, see [FZ10]. Note that beyond connectedness, [CFZ11] provides an explicit formula for the cardinality of $\mathrm{ST}([k-2],k)$.

1.4 Organisation and sketch of proof

We start by giving all definitions related to square-tiled surfaces and shears in Section 2. This section also contains background on Abelian and quadratic differentials and the definition of the weighted stable graph of a square-tiled surface, that encodes the structure of its cylinders. In Section 3, we focus on the square-tiled surfaces of genus 0 and show how they can be connected to some path-like square-tiled surface, which contains only one horizontal cylinder. We derive from the existence of these path-like square-tiled surfaces the lower bound of Theorem 1.7. Then in Section 4, we conclude the proof of Theorem 1.7 by showing that all these path-like configurations are related by cylinder shears. To do so, we show that they are all equivalent to a canonical one, by progressively introducing structure in the path-like configuration. Finally, we address in Section 5 the case of Abelian hyperelliptic square-tiled surfaces by reducing to square-tiled surfaces of genus zero, thereby proving Theorem 1.6.

To conclude, we discuss in Section 6 several works related to our result as well as possible extensions.

Acknowledgments

The second author was partially supported by the Polish National Science Centre under grant no. 2019/34/E/ST6/00443.
Both authors benefited from the ANR project Modiff ANR-19-CE40-0003-01.
Both authors thank Luke Jeffreys for organizing the workshop *Square-tiled surfaces: a classification of cylinder block shearing orbits* at the Heilbronn Institute in Bristol in summer 2023 during which we had the opportunity to discuss this work (see https://heilbronn.ac.uk/2023/06/12/frg-square-tiled-surfaces/).

2 Square-tiled surfaces

2.1 Square-tiled surfaces and their dual tricoloured cubic graphs

Recall that a square-tiled surface is a quadrangulation of a connected surface whose edges are assigned a 2-colouring corresponding to the horizontal and vertical directions.

Let us introduce a natural encoding of a square-tiled surface that we will use as our main combinatorial definition. We fix an arbitrary labelling of the bottom-left and top-right corners of each square by the elements of $[n] \coloneqq \{1, \dots n\}$ where n is twice the number of squares. We define τ_R, τ_G, τ_B three involutions without fixed points on $[n]$, such that τ_R, τ_G and τ_B record respectively the adjacencies of the labels across the horizontal edges, inside a square and across the vertical edges. By drawing diagonals in each square we turn the square-tiled surface τ into a triangulation. In this triangulation, the involution τ_G encodes adjacencies along the diagonal. We always use the following colour convention for the edges (see Figure 5):

- horizontal edges (ie the transpositions in the cycle decomposition of τ_R) are red,
- diagonal edges (ie the transpositions of τ_G) are green,

- vertical edges (ie the transpositions of τ_B) are blue.

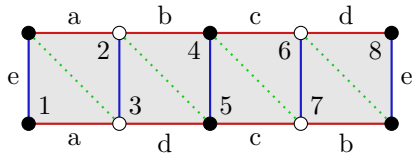

$\tau_R = (1,2)(3,8)(5,6)(7,4)$
$\tau_G = (1,2)(3,4)(5,6)(7,8)$
$\tau_B = (2,3)(4,5)(6,7)(8,1)$

(a) A labelling of the square-tiled surface from Figure 4a.

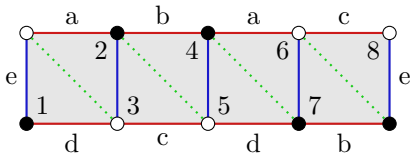

$\tau_R = (1,5)(2,6)(3,8)(7,4)$
$\tau_G = (1,2)(3,4)(5,6)(7,8)$
$\tau_B = (2,3)(4,5)(6,7)(8,1)$

(b) A labelling of the square-tiled surface from Figure 4b.

Figure 5: Labellings of the two square-tiled surfaces from Figure 4.

Conversely, starting from a triple of involutions without fixed points $\tau = (\tau_R, \tau_G, \tau_B)$ such that they act transitively on $[n]$, one can build a square-tiled surface. If the action is not transitive, then the resulting surface is not connected.

We now introduce folded edges. Instead of using bicoloured squares as building blocks we use tricoloured triangles (that should be thought as "half" of a square cut along its diagonal). We pick n copies of them that we label from 1 to n. Then we consider three involutions (possibly with fixed points) τ_R, τ_G and τ_B that determine the gluings of the edges with colours respectively R, G and B. If j is a fixed point of τ_i then the edge coloured i on the j-th triangle is glued to itself by a 180-degree rotation (see Figure 6). From now on, we will use the term square-tiled surface to refer to a triple of involutions (possibly with fixed points) that act transitively on $[n]$ and we will denote $S(\tau)$ the tricoloured triangulation we have just constructed (see Figure 6a). We call n the *number of triangles* in $S(\tau)$. A *red half-edge* (respectively *green half-edge* and *blue half-edge*) is a fixed point of τ_R (resp. τ_G and τ_B).

We denote $S^*(\tau)$ the *tricoloured cubic graph* dual to the triangulation $S(\tau)$ (see Figure 6b). The graph $S^*(\tau)$ has vertex set $\{1, \dots, n\}$. There is a red, green or blue edge between i and j if respectively (i, j) is a transposition in the cycle decomposition of τ_R, τ_G or τ_B. And there is a red, green or blue half-edge at i if it is a fixed point of respectively τ_R, τ_G or τ_B. The graph $S^*(\tau)$ is naturally embedded in the square-tiled surface $S(\tau)$ and at every vertex the cyclic order colours of the three adjacent edges or half-edges are counter-clockwise in the order red then green then blue.

We call i-*faces* of $S^*(\tau)$ or $3i$-gons the faces of $S^*(\tau)$ of degree $3i$. For example, there is one 2-face, or also called hexagon, and one 3-face in Figure 6b. Note that the i-faces are dual to the vertices of degree $3i$ in $S(\tau)$.

Given a triangulation $S(\tau)$ with n triangles and $\sigma \in S_n$ we denote $\tau^\sigma = (\sigma\tau_R\sigma^{-1}, \sigma\tau_G\sigma^{-1}, \sigma\tau_B\sigma^{-1})$. The triangulated square-tiled surface $S(\tau^\sigma)$ corresponds to the same underlying triangulation as $S(\tau)$ but where the labels of the triangles have been permuted by σ. We say that two square-tiled surfaces τ and τ' are *isomorphic* if they have the same number of triangles n and there exists a permutation $\sigma \in S_n$ such that $\tau' = \tau^\sigma$, in other words, $S(\tau)$ is isomorphic to $S(\tau')$.

The *profile* of τ is the pair (μ, k), where μ is the integer partition counting the i-faces for any i, while k is the total number of half-edges. We use the standard notation $\mu = [1^{\mu_1}, 2^{\mu_2}, \dots]$ to denote 1 repeated μ_1 times, 2 repeated μ_2 times, etc. We denote $\mathrm{ST}(\mu, k)$ the set of isomorphism classes of square-tiled surfaces with profile (μ, k). Let us note that Euler's characteristic

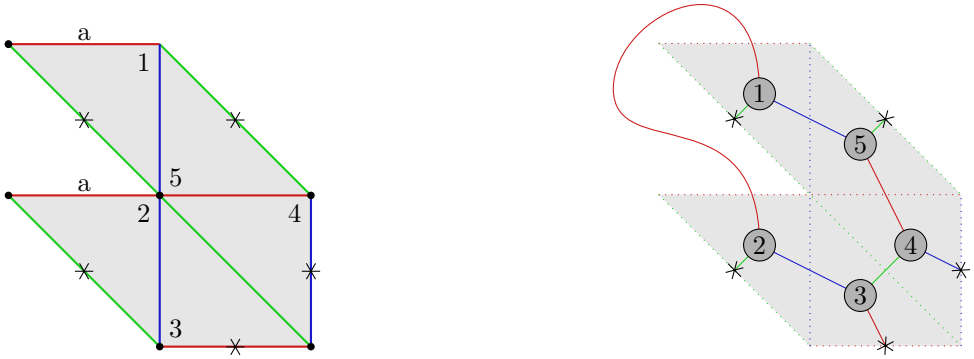

(a) The triangulation $S(\tau)$ encoded by τ (b) Its dual tricoloured cubic graph $S^*(\tau)$

Figure 6: A square-tiled surface τ represented by its tricoloured triangulation and its tricoloured cubic graph. We have $\tau_R = (1,2)$, $\tau_G = (3,4)$ and $\tau_B = (1,5)(2,3)$. In particular, τ is of genus 0 and has profile $([2,3],5)$. When drawing the tricoloured triangulation of a square-tiled surface τ, we will mark with a star the edges glued to themselves, that is, the fix points of τ. Likewise, we will represent the half-edges in $S^*(\tau)$ with a star at their endpoint.

allows to compute the genus g of a square-tiled surface from its profile (μ, k) by

$$4g - 4 = \sum_i \mu_i \cdot (i-2) - k. \tag{2}$$

Let us also note that the number of triangles n satisfies

$$n = \sum_{i \geqslant 1} \mu_i \cdot i. \tag{3}$$

A square-tiled surface τ is *Abelian* if there exists a non-trivial partition $A_+ \sqcup A_- = [n]$ such that $\tau_i(A_+) = A_-$ for each $i \in \{R, G, B\}$. Equivalently, it is Abelian if it has no half-edges and its dual graph $S^*(\tau)$ is bipartite. A square-tiled surface which is not Abelian is called *quadratic*. We denote $\mathrm{ST}_{Ab}(\mu, k)$ and $\mathrm{ST}_{quad}(\mu, k)$ respectively the Abelian and quadratic square-tiled surfaces of profile (μ, k). By definition $\mathrm{ST}(\mu, k)$ is the disjoint union of $\mathrm{ST}_{Ab}(\mu, k)$ and $\mathrm{ST}_{quad}(\mu, k)$.

We finish this introduction to square tiled-surfaces by giving a parity restriction on the profile.

Lemma 2.1. *Let τ be a square-tiled surface on $[n]$ with profile (μ, k). Then we have*

$$3n - k \equiv 2 \sum_{i \geqslant 1} \mu_{2i} \mod 4. \tag{4}$$

Proof. The faces of $S^*(\tau)$ are in bijection with the cycles of the product $\tau_R\tau_G\tau_B$ whose cycle type is μ. We claim that (4) follows from the signature morphism $\epsilon : (S_n, \cdot) \to (\mathbb{Z}/2\mathbb{Z}, +)$ which gives $\epsilon(\tau_R) + \epsilon(\tau_G) + \epsilon(\tau_B) = \epsilon(\mu)$. Indeed $\epsilon(\tau_i) = \frac{n-k_i}{2} \mod 2$ where k_i is the number of fixed points of τ_i, because τ_i is an involution. Hence $\epsilon(\tau_R) + \epsilon(\tau_G) + \epsilon(\tau_B) = \frac{3n-k}{2} \mod 2$. And we have $\epsilon(\mu) = \sum_{i \geqslant 1} \mu_{2i} \mod 2$ which concludes the proof of the lemma. □

2.2 Cylinder shear

We now introduce formally the cylinder shears on tricoloured cubic graphs $S^*(\tau)$. They generalise the induction defined in the case of trees in [CFZ11].

Let $\tau = (\tau_R, \tau_G, \tau_B)$ be a square-tiled surface. Let us consider a pair of colours $\{i, j\} \subset \{R, G, B\}$. A $\{i, j\}$-*component* is a connected component of the subgraph of $S^*(\tau)$ in which we only keep the edges coloured i or j. More combinatorially, these correspond to the orbits of the subgroup $\langle \tau_i, \tau_j \rangle$. Because the graph induced on $\{i, j\}$ has degree 2 and possibly half-edges, each $\{i, j\}$-component is either a path or a cycle and we call them respectively $\{i, j\}$-*path* or $\{i, j\}$-*cycle*.

Let $c \subset [n]$ be a $\{R, G\}$-component. Let $c_R \coloneqq \tau_R|_c$ and $c_G \coloneqq \tau_G|_c$ be the restrictions of τ_R and τ_G to c (by definition τ_R and τ_G preserve c). The (R, G)-*shear along* c is the square-tiled surface $\mathrm{Shear}_{c,R,G}(\tau) \coloneqq (\tau_R \cdot c_R \cdot c_G, \tau_G \cdot c_R \cdot c_G, \tau_B)$.

More graphically, the (R, G)-shear along c affects $S^*(\tau)$ by switching colours R and G in c and sliding all adjacent edges coloured B, see Figure 7. Note that τ_B remains unchanged under this operation.

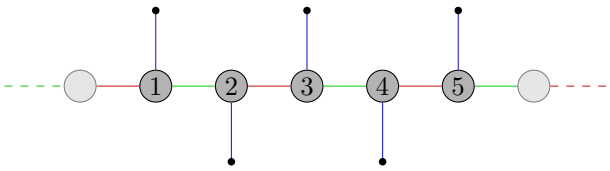

(a) A piece of a $\{R, G\}$-component of a square-tiled surface τ (represented by its dual tricoloured cubic graph) and its neighbourhood.

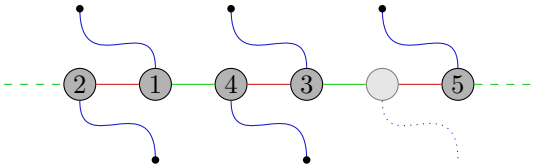

(b) A piece of the square-tiled $\mathrm{Shear}_{c,R,G}(\tau)$ with the same vertex position as in Figure 7a.

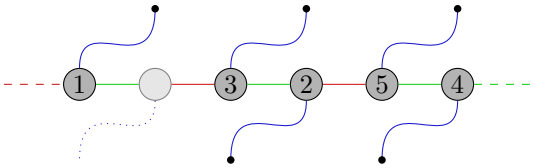

(c) A piece of the square-tiled $\mathrm{Shear}_{c,G,R}(\tau)$ with the same vertex position as in Figure 7a.

Figure 7: A piece of a $\{R, G\}$-component and its neighbourhood before and after a (R, G)-shear.

Let $\tau' = \mathrm{Shear}_{c,R,G}(\tau)$. The vertices of $S^*(\tau)$ and $S^*(\tau')$ are $[n]$ and are hence in natural bijection. Moreover, there is a natural bijection between the edges of $S^*(\tau)$ and $S^*(\tau')$ that preserves the colours of all edges but those in the component c, which are exchanged. As we already mentioned, blue edges remain unchanged. Similarly, green and red edges outside of c remain unchanged. We only need to discuss how to match the (red and green) edges of $S^*(\tau)$ and $S^*(\tau')$ inside c. Recall that on c we have

$$\tau'_R|_c = \tau_G|_c \qquad \tau'_G|c = (\tau_G \cdot \tau_R \cdot \tau_G)|_c$$

In particular a green edge (corresponding to transposition of τ_G) or half-edge (corresponding to a fixed point of τ_G) of $S^*(\tau)$ becomes a red edge or respectively half-egde of $S^*(\tau')$. And we map a red edge (ij) or half-edge (i) of $S^*(\tau)$ to the green edge $(\tau_G(i)\tau_G(j)) = (ij)^{\tau_G}$ or respectively half-edge $(\tau_G(i)) = (i)^{\tau_G}$.

We define similarly (i,j)-shears for any pair of colours in $\{R,G,B\}$ and we naturally extend the definition of $\mathrm{Shear}_{c,i,j}$ when c is a union of $\{i,j\}$-components. Note that $\mathrm{Shear}_{c,R,G}$ and $\mathrm{Shear}_{c,G,R}$ are different operations (they differ on the image of τ_B) and we get 6 possible shears. We call *horizontal cylinders* the $\{G,B\}$-components and *horizontal shears* the (B,G) and (G,B)-shears. Similarly, we call *vertical cylinders* the $\{R,G\}$-components and *vertical shears* the (R,G) and (G,R)-shears. Note that one could similarly define *diagonal shears* as the (R,B) and (B,R)-shears, however we will avoid them for the following reasons. The geometric interpretation of a diagonal cylinder on the quadrangulation corresponding to a square-tiled surface is unclear and there is no apparent reason to favour one diagonal over the other. Moreover, these shears can be realised by a sequence of horizontal and vertical shears whose length is linear in the size of the diagonal cylinder.

We now prove that shears preserve the stratum and stabilise the Abelian components.

Lemma 2.2. *Let τ be a square-tiled surface, i, j two colours in $\{R,G,B\}$ and c a $\{i,j\}$-component. Let $\tau' = \mathrm{Shear}_{c,i,j}(\tau)$ be the square-tiled surface obtained after a cylinder shear. Then*

1. *$\tau_R \cdot \tau_G \cdot \tau_B = \tau'_R \cdot \tau'_G \cdot \tau'_R$,*
2. *τ and τ' have the same profile,*
3. *τ is Abelian if and only if τ' is.*

Proof. We only consider the case of $i = R$ and $j = G$ the other cases being similar.

Let $\tau = (\tau_R, \tau_G, \tau_B)$ be a square-tiled surface and $\tau' = (\tau'_R, \tau'_G, \tau'_B) = \mathrm{Shear}_{c,R,G}(\tau)$. Then

$$\tau'_R \cdot \tau'_G \cdot \tau'_B = (\tau_R \cdot c_R \cdot c_G) \cdot (\tau_G \cdot c_R \cdot c_G) \cdot \tau_B = \tau_R \cdot (c_R \cdot c_G \cdot \tau_G \cdot c_R \cdot c_G) \cdot \tau_B$$

Now we note that $c_R \cdot c_G \cdot \tau_G = \tau_G \cdot c_G \cdot c_R$. Indeed, outside of c both sides are equal to τ_G and in c both sides are equal to c_R. In particular, the rightmost term in the chain of equalities simplifies to $\tau_R \cdot \tau_G \cdot \tau_B$ and concludes the proof of the first item.

Let (μ, k) and (μ', k') be the profiles of respectively τ and τ'. Recall that (μ, k) is the pair made of the integer partition μ associated to the conjugacy class of the product $\tau_R\tau_G\tau_B$ and the integer k which is the sum of the number of fixed points in τ_R, τ_G and τ_B. By the previous item we have that $\mu = \mu'$. Next, the number of fixed points of $\tau_B = \tau'_B$ are identical. Also, since τ_R and τ_G are unchanged outside of c, the number of fixed points up to the ones in c coincide. We show that the sum of the number of green and red fixed points in c are identical. Indeed, we have $\tau'_R|_c = \tau_G|_c$ and $\tau'_G|_c = (\tau_G \cdot \tau_R \cdot \tau_G)|_c$ and hence the number of red and green fixed points are exchanged in c. This shows that the total number of fixed points remains unchanged.

Finally, if τ admits an invariant partition $A_+ \sqcup A_-$ then the same partition is invariant by τ'. □

Next, we immediately see from the definition that $\mathrm{Shear}_{c,R,G}$ and $\mathrm{Shear}_{c,G,R}$ are inverse of each other.

Lemma 2.3. *Let τ be a tricoloured cubic graph, i, j two colours in $\{R,G,B\}$ and c a $\{i,j\}$-component. Then c is also a $\{i,j\}$-component in $\mathrm{Shear}_{c,i,j}(\tau)$ and $\mathrm{Shear}_{c,j,i}(\mathrm{Shear}_{c,i,j}(\tau)) = \tau$.*

Finally, let us conclude with an analogy between cylinder shears in square-tiled surfaces and a reconfiguration problem on graph colourings. An *edge-colouring* of a graph is an assignment of colours to the edges, such that incident edges receive different colours. A Kempe

change consists in swapping two colours in a maximal bichromatic component of the colouring. So a cylinder shear comes down to performing a Kempe change on the 3-edge-colouring of $S^*(\tau)$, before sliding the incident edges to preserve the cyclic ordering of the colours around the vertices of $S^*(\tau)$.

2.3 Abelian and quadratic differentials

We now introduce Abelian and quadratic differentials on Riemann surfaces and their associated moduli spaces. We explain how Abelian and quadratic square-tiled surfaces are particular cases of differentials and how a cylinder shear can be realised as a continuous path in the moduli space. The main consequence of this fact is the proof of Proposition 1.5. Beyond the proof of this proposition, the definitions in this section will be used only in Section 5.

For a more detailed introduction to Abelian and quadratic differentials, we refer the reader to the survey [Zor06] and the book [AM24].

One often uses the term *translation surface* to refer to a compact Riemann surface endowed with a non-zero Abelian differential (or equivalently a holomorphic one-form). The reason is that the most elementary way to define such object is by considering a finite collection of Euclidean polygons whose edges are identified by translations (see [Zor06, Section 1.2] and [AM24, Chapter 2]). The Abelian square-tiled surfaces we consider in this article are indeed particular cases of translation surfaces. More precisely, let $\tau = (\tau_R, \tau_G, \tau_B)$ be an Abelian square-tiled surface on $[n]$ where n is twice the number of quadrilaterals. Let $A^+ \sqcup A^-$ be a τ-invariant bipartition of $[n]$. We consider $n/2$ copies of unit squares with bottom left labelled with elements of A^+ and from now on, we identify the squares with their labels in A^+. Recall that $[n]$ corresponds to the triangles and that the "other half" of the bottom left triangle labelled $i \in A^+$ is labelled $\tau_G(i) \in A^-$ so that a square is made of two triangles. Now we glue the right side of the square labelled $i \in A^+$ to the left side of $\tau_R(\tau_G(i))$ and its top side to the bottom side of $\tau_B(\tau_G(i))$. Note that there is one ambiguity in the construction which is the choice of the bipartition. If the partitions A^+ and A^- are swapped, we obtain a (possibly different) translation surface built from squares that are all rotated by 180 degrees. In other words, we associate to an Abelian square-tiled surface τ a translation surface up to rotation by 180 degrees that we denote by $\pm S$.

Two translation surfaces S and S' are *isomorphic* if one can obtain one from the other by a sequence of cutting and gluing operations on the polygons (see [AM24, Section 2.5.4]).

Lemma 2.4. *Let τ and τ' be two Abelian square-tiled surfaces on $[n]$. Then τ and τ' are isomorphic (for the definition from Subsection 2.1) if and only if the associated translation surfaces $\pm S$ and $\pm S'$ are isomorphic.*

In order to prove Lemma 2.4, we need to introduce two additional definitions. A translation surface S is naturally a metric space where the distance is induced from the Euclidean distance on each polygon forming S. Endowed with this metric, each point on a translation surface has a neighbourhood which is isometric to the neighbourhood of the apex of a flat cone of angle $(1+k)2\pi$ where k is a non-negative integer. When $k = 0$ such a point is called *regular*. For $k > 0$, such a point is called a *conical singularity of angle* $(1+k)2\pi$ and k is called the *excess*. Any point inside a polygon or inside an edge is regular. However, the vertices might be regular or a conical singularity. For example, the corners of the squares in Figure 4a correspond to two points on the associated translation surface. Both of these points have angle 4π, in other words they have excess 1.

To S we associate the integer partition $\kappa = [1^{\kappa_1}, 2^{\kappa_2}, \ldots]$ where κ_i is the number of conical singularities of excess i on S. The genus of S is related to κ by the following Euler's formula

$\sum \mu_i \cdot i = 2g - 2$. For a square-tiled surface $S(\tau)$ one can obtain the integer partition κ from its profile μ as $\kappa = [1^{\mu_4}, 2^{\mu_6}, \ldots]$.

Beyond the metric, one can make sense of *straight line segments* in S and associate to a straight line segment a *direction*. One uses the standard Euclidean notion in each polygon of S and such definition can be made global since the gluings are done by translation. Namely, segments can be defined on each polygon S is made of and pieces of segments ending in middle of edges of the polygons can be glued together to form longer segments. In a square-tiled surfaces, the red, blue and green edges are examples of horizontal segments, vertical segments and segments of slope -1. A *saddle connection* in S is a segment both of whose endpoints are conical singularities (possibly the same).

We are now ready to prove Lemma 2.4.

Proof. Let us first remark that the number of triangles n of τ and τ' is twice the number of squares, which is the areas of S and S'.

It is clear that if τ and τ' are isomorphic then $\pm S$ and $\pm S'$ are isomorphic. Indeed, the labelling of the squares is irrelevant in the geometric structure.

We now focus on the other implication. Namely, assume that S and S' are isomorphic as translation surfaces. Let us first remark that the isomorphism of translation surfaces preserves area and singularities. Hence the number of squares in τ and τ' are identical as well as the vector of excesses κ and κ'.

In order to prove that τ and τ' are isomorphic we show that the triangulation of S induced by τ can be reconstructed from the geometric structure of S only. It will result that if S and S' are isomorphic, then the underlying triangulations are isomorphic and so are τ and τ'.

Let us first assume that S has at least one conical singularity (ie it is not a torus in $\mathcal{H}(\emptyset)$). We consider in S the horizontal and vertical saddle connections issued from these conical singularities. These saddle connections are respectively unions of red and blue edges of the underlying triangulation. The lengths of each of these saddle connections is integral and we mark the regular points at each unit length along them. These marked points are vertices of τ. We then consider horizontal and vertical saddle connections issued from these marked points and iterate the process until there is no new segment discovered. Each time a new regular point is marked it is a vertex of τ, and each horizontal and vertical saddle connection built is a subset of the red and blue edges of the triangulation respectively. By connectedness of the triangulation, all red and blue edges are recovered in this way. The red and blue edges form a square tiling and one obtains the green edges by picking the north-west to south-east diagonals (which is the same diagonal on S and $-S$). This concludes the case when S is not a flat torus.

We now consider the case of S being a flat torus. In this case S is isomorphic to a quotient $\mathbb{R}^2/\Lambda$ where Λ is a lattice and hence admits a group structure. For each element $x \in \mathbb{R}^2/\Lambda$ the translation $y \mapsto x + y$ is an isomorphism of S. In particular, given any two points x and y on S there exists a unique isomorphism of S that maps x to y (the translation by $y - x$). Let us choose an arbitrary point in S that we declare as a marked point. By the previous discussion, the choice of such point is geometrically irrelevant. From there, we can perform the construction of the previous paragraph starting at this regular marked point. We obtain a triangulation which is isomorphic to the one obtained from τ. □

The set of isomorphism classes of the translation surfaces with fixed vector κ forms an algebraic variety, in particular a topological space which is denoted $\mathcal{H}(\kappa)$ (see [Zor06, Section 3.1] and [AM24, Chapter 3]). It follows that $\mathcal{H}(\kappa)$ has finitely many connected components, which are also path-connected. These connected components have been classified in [KZ03]. The

topology of $\mathcal{H}(\kappa)$ is easy to describe: two surfaces are nearby if they are obtained by the same gluing patterns of nearby collections of polygons.

Lemma 2.5. *Let S in $\mathcal{H}(\kappa)$ be the translation surface associated to an Abelian square-tiled surface τ. Let S' be the translation surface associated to the square-tiled surface $\tau' = \mathrm{Shear}_{c,i,j}(\tau)$ obtained after a cylinder shear, where c is some $\{i,j\}$-component of τ. Then S' belongs to $\mathcal{H}(\kappa)$ and there is a continuous path from S to S' in $\mathcal{H}(\kappa)$.*

Proof. By Lemma 2.2, the profile of τ' is the same as the one of τ and τ' is Abelian. Hence the translation surface S' belongs to the same stratum $\mathcal{H}(\kappa)$ as S'. Though, we will also obtain this fact from the explicit construction of a continuous path from S to S'.

Now, our goal is to build a continuous path of translation surfaces $\{S_t\}_{t\in[0,1]}$ inside $\mathcal{H}(\kappa)$ such that $S_0 = S$ and $S_1 = S'$. The $\{i,j\}$-component c in τ corresponds to a horizontal cylinder in the translation surface S. More precisely, the closure of the subset of squares corresponding to this $\{i,j\}$-component forms a cylinder of height one. We define the surface S_t to be the translation surface built from an identical number of quadrilaterals where the quadrilaterals outside of c remains squares but the one in c are the "slanted" quadrilaterals with vertices $[(0,0),(1,0),(1+t,1),(t,0)]$. It is easy to notice that S_1 and S' are indeed isomorphic. □

We now turn to quadratic differentials on Riemann surfaces which are sometimes referred to as *half-translation surfaces*. One can build a half-translation surface by taking finitely many Euclidean polygons and gluing their edges using translations and 180-degree rotations (see [Zor06, Section 8.1] and [AM24, Section 2.7]). Similarly to the Abelian case, we associate to a half-translation surface an integer partition with parts in $\{-1,1,2,3,\dots\}$ denoted $\kappa = [(-1)^{\kappa_{-1}}, 1^{\kappa_1}, \dots]$ such that there are κ_i singularities of angle $(2+i)\pi$. Euler's formula in the quadratic case reads $\sum i\cdot\kappa_i = 4g-4$. Similarly to the Abelian case, there exist strata $\mathcal{Q}(\kappa)$ that consist of quadratic strata that are not squares of Abelian differentials.

Given a quadratic square-tiled surface in $\mathrm{ST}_{quad}(\mu,k)$ on $[n]$, one obtains a half-translation surface built from n right-angled triangles (which should be thought of as "half squares"). The vector κ associated to this half-translation surface has integer partition $[(-1)^{k+\mu_1}, 1^{\mu_3}, 2^{\mu_4}, \dots]$. Note that both half-edges (corresponding to k) and vertices of degree 1 (corresponding to μ_1) give rise to singularities of angle π.

Similarly to Lemma 2.5, we have the following.

Lemma 2.6. *Let S in $\mathcal{Q}(\kappa)$ be the half-translation surface associated to a quadratic square-tiled surface τ. Let S' be the half-translation surface associated to the square-tiled surface $\tau' = \mathrm{Shear}_{c,i,j}(\tau)$ obtained after a cylinder shear, where c is some $\{i,j\}$-component of τ. Then S' belongs to $\mathcal{Q}(\kappa)$ and there is a continuous path from S to S' in $\mathcal{Q}(\kappa)$.*

Proof. By Lemma 2.2, τ' is quadratic and its profile is the same as the one of τ. Hence, the half-translation surface S' belongs to the same stratum $\mathcal{Q}(\kappa)$ as S'.

It is straightforward to extend the proof of Lemma 2.5 to the quadratic case when c is a cycle. In the case where c is a path, the union of triangles corresponding to c in S is still a horizontal cylinder, though of height $1/2$. The same shearing construction works. □

We can now prove Proposition 1.5, which states that the connected components induced by the cylinder shears refine the connected components of the strata of the moduli space of quadratic differentials.

Proof of Proposition 1.5. By Lemma 2.5 and Lemma 2.6 cylinder shears can be realised as a continuous path in respectively $\mathcal{H}(\kappa)$ and $\mathcal{Q}(\kappa)$. In particular, if τ belongs to a given connected component of $\mathcal{H}(\kappa)$ or $\mathcal{Q}(\kappa)$ its image under a cylinder shear belongs to the same connected component. □

2.4 Cylinder decomposition and weighted stable graphs

We introduce now the weighted stable graph of a square-tiled surface that encodes the geometry of its $\{G, B\}$-components. It follows closely the notions in [DGZZ20, Section 4.7] and [DGZZ21, Section 2.2]. The weighted stable graph will be the main tool in Section 3 but will not be used elsewhere.

Let τ be a square-tiled surface. Recall from Subsection 2.3 that when viewed as the gluing of right-angled triangles, $S(\tau)$ carries the geometry of an Abelian or quadratic differential. In such a surface, it makes sense to consider horizontal segments: these are continuous paths that are horizontal in every triangle. The *critical graph* of $S(\tau)$ is the graph embedded in the surface $S(\tau)$ whose vertices are the singularities of $S(\tau)$ (i.e. the union of vertices of τ whose degree is different from 6 and the mid-points of half-edges) and its edges are the union of all horizontal segments ending at these singularities. A connected component of the critical graph is a saddle connection that either consists entirely of red edges or half-edges of $S(\tau)$ or connects two conical singularities of angle π. These saddle connections are in bijection with the horizontal cylinders in $S^*(\tau)$.

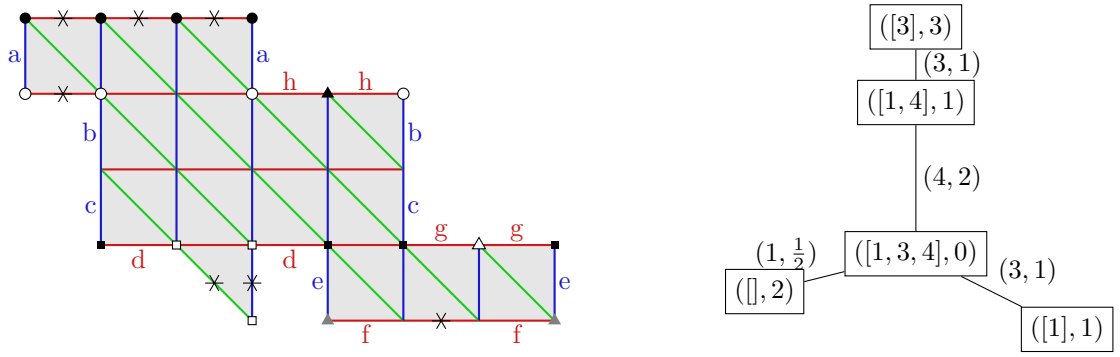

(a) A spherical square-tiled surface in $\mathrm{ST}_{quad}([1^3, 2^6, 3^2, 4^2], 7)$.

(b) The weighted stable graph of Figure 8a.

Figure 8: A square-tiled surface $S(\tau)$ and its weighted stable graphs $\Gamma(\tau)$.

The *weighted stable graph* associated to τ is the multigraph $\Gamma(\tau)$ together with vertex decorations $(\mu^{(v)}, k^{(v)})$ for each vertex $v \in V(\Gamma(\tau))$ and edge decorations (w_e, h_e) for each edge $e \in E(\Gamma(\tau))$ built as follows.

- $V(\tau)$ is the set of connected components of the critical graph of $S(\tau)$; the vertex decoration $(\mu^{(v)}, k^{(v)})$ associated to a component records the singularity pattern of that component ignoring regular vertices (corresponding to μ_2),
- $E(\tau)$ is the set of cylinders, i.e. the connected components of $S(\tau)$ minus the critical graph. The two ends of an edge are the two connected components of the critical graph to which the boundaries of cylinder are glued to; the edge decoration $(w_e, h_e) \in \mathbb{Z}_{>0} \times \frac{1}{2}\mathbb{Z}_{>0}$ records the width and height of the cylinder. Note that this allows loops.

By construction

- the union of the vertex decorations $(\mu^{(v)}, k^{(v)})$ is the *reduced profile* of τ, that is the profile μ of τ where the singularities corresponding to μ_2 are omitted.
- the number of triangles $n = \sum_{i \geqslant 0} \mu_i$ of $S(\tau)$ satisfies $\sum_{e \in E(\Gamma)} w_e \cdot h_e = \frac{n}{2}$.

Let us terminate this subsection with three remarks. First, we note that one can read the genus of $S(\tau)$ from $\Gamma(\tau)$. Namely, to each vertex $v \in V(\Gamma)$ one can associate the genus of the corresponding singular layer $g^{(v)}$ which is obtained from the vertex decoration and the degree of v in $\Gamma(\tau)$ as

$$4g^{(v)} - 4 = \sum_i \mu_i^{(v)} \cdot (i-2) - k^{(v)} - 2\deg(v).$$

Then the genus of the surface $S(\tau)$ is $\sum_{v\in\Gamma(\tau)} g^{(v)} + |E(\Gamma(\tau))| - |V(\Gamma(\tau))| + 1$. In particular, for a spherical square-tiled surfaces, $\Gamma(\tau)$ is always a tree.

Secondly, if $S(\tau)$ and $S(\tau')$ are two square-tiled surfaces that differ by some horizontal shears then their weighted stable graphs $\Gamma(\tau)$ and $\Gamma(\tau')$ are isomorphic.

Finally, if $S(\tau)$ is a square-tiled surface and c_1 and c_2 are two $\{G, B\}$-components that correspond to the same edge in $\Gamma(\tau)$ then the associated cylinder shears produce isomorphic square-tiled surfaces (see Figure 9).

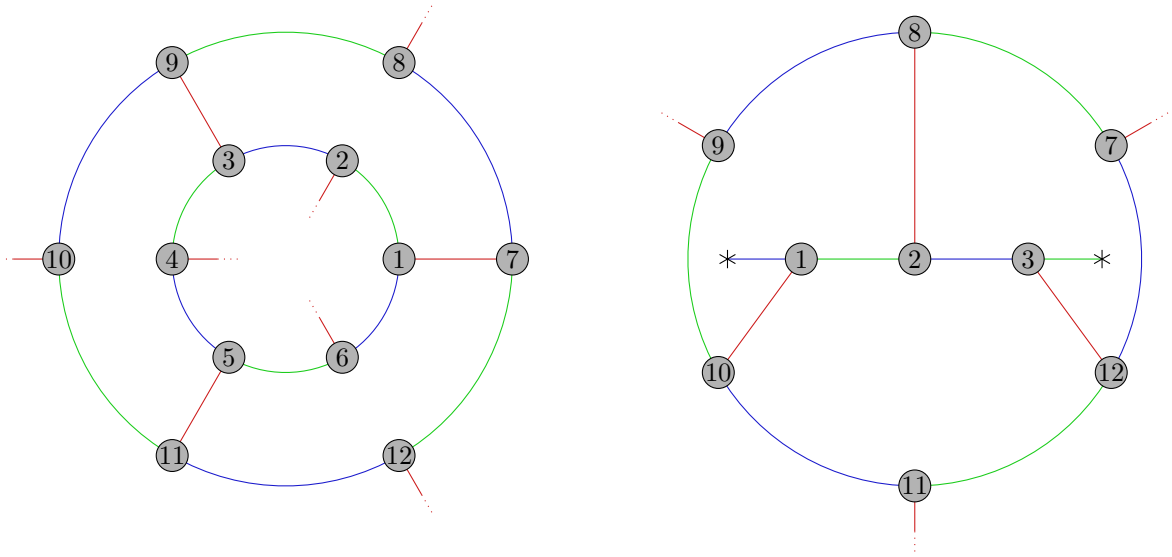

(a) Two $\{G, B\}$-cycles of length 6 (separated by three hexagons) whose shearing produces isomorphic square-tiled surfaces.

(b) A $\{G, B\}$-path of length 3 and a $\{G, B\}$-cycle of length 6 whose shearing produces isomorphic square-tiled surfaces.

Figure 9: Equivalence of cylinder shears.

3 Connecting to path-like configurations

In this section, we focus on the square-tiled surfaces of genus 0, also called *spherical square-tiled surfaces*. These square-tiled surfaces are exactly those whose profile is *spherical*, i.e. satisfies $\sum_i (i-2)\mu_i = k - 4$. We will assume that it is the case in this whole section.

3.1 Path-like configurations

A square-tiled surface is called a *path-like configuration* if it has a single horizontal cylinder (that is, a $\{G, B\}$-component) which furthermore is a path. The path-like square-tiled surfaces correspond to some specific Jenkins-Strebel differentials appearing in [Zor08] and to the one-cylinder square-tiled surfaces studied in [DGZ+20].

Note that if (μ, k) is the profile of a path-like configuration then necessarily $k \geqslant 2$ because of the two ends of the path. One important result of this subsection is that this condition is the only restriction on the profile for the existence of path-like square-tiled surfaces.

Theorem 3.1. *Let (μ, k) be a spherical profile, with $k \geqslant 2$. Then there exists a path-like configuration with profile (μ, k).*

In order to prove Theorem 3.1 we construct a surjective map between path-like configurations and certain decorated plane trees, that we define below. This map will be used in Section 4 to reconfigure path-like square-tiled surfaces.

A *decorated plane tree* is a pair (T, L) where T is a tree embedded in the sphere and L is a subset of the leaves of T. We say that (T, L) has *profile* (μ, ℓ) if L has size ℓ and the vertices of T not in L have degrees given by the integer partition μ. We will call *L-leaves* the leaves in L and *$\overline{L}$-leaves* the other leaves. The *perimeter* of a decorated plane tree is its number of edges incident to an L-leaf plus twice the number of other edges.

Let τ be a path-like square-tiled surface. We explain how to associate to τ its decorated plane tree. The vertex set of T contains the vertices of the surface $S(\tau)$, together with the set L containing one vertex for each half-edge of $S(\tau)$. To obtain T, it suffices to keep only the red edges of $S(\tau)$, and to replace the red half-edges by an edge connecting its endpoint to a L-leaf. Note that (T, L) can also be defined by taking the dual of the red edges in the cubic graph $S^*(\tau)$. The main result of this subsection and argument in the proof of Theorem 3.1 is the following relationship between path-like configurations and decorated plane trees.

Theorem 3.2. *Let (μ, k) be a spherical profile with $k \geqslant 2$. Then the map which takes a path-like configuration with profile (μ, k) to its decorated plane tree is a surjection onto decorated plane trees with profile $(\mu, k-2)$. Furthermore, for each decorated plane tree (T, L) with profile $(\mu, k-2)$ the corresponding preimage of path-like configurations is made of a single orbit under the horizontal shears.*

Proof. Let τ be a path-like configuration with profile (μ, k). We first prove that its image is indeed a decorated plane tree. The only thing to prove is that T is indeed a tree. As τ is spherical and $S(\tau)$ has only one $\{G, B\}$-component that is a path, hence not separating, the complement of T in the sphere is indeed a disk.

To obtain the surjectivity, we now explain how to build the tricoloured cubic graph dual to a path-like configuration that maps to a given pair (T, L) with profile $(\mu, k-2)$. We first consider the arch configuration dual to (T, L) on a disk as in Figure 10. Here by *arch configuration* we mean a choice of a non-intersecting matching (or involution) on cyclically ordered points. An arch configuration has a geometric realization as a union of arcs of circles (for each pair of the matching) and segments with one end on the boundary (for points not in the matching). Then in another disk, we consider a $\{G, B\}$-path on n vertices and add red segments going to the boundary as the red picture in Figure 10 where n is the perimeter of (T, L). Finally we obtain a spherical square-tiled surface by gluing together the two disks as in Figure 11. Note that there are n possible choices of gluings and each of them gives a square-tiled surface with the same dual decorated plane tree (T, L).

We now prove that the set of square-tiled surfaces with decorated plane tree (T, L) forms a single orbit under horizontal shears. Let $S^*(\tau)$ be a tricoloured cubic graph dual to a given τ with decorated plane tree (T, L). We will mark (T, L) to track the position of the $\{G, B\}$-path of $S^*(\tau)$ compared to the red edges. We associate a *marking site* to each endpoint of the red edges of $S^*(\tau)$ (each half-edge receives only one marking site instead of two). In (T, L), this corresponds to placing a marking site on each edge of T adjacent to an L-leaf and one on each

side of the other edges. We now need to distinguish two cases depending on the parity of the perimeter of (T, L), that is the number of marking sites in (T, L). Note that (T, L) has an even perimeter if and only if the half-edges at the endpoint of the $\{G, B\}$-path of $S^*(\tau)$ (and all other preimages of (T, L)) have identical colours.

Assume that they have distinct colours, this corresponds to the case where (T, L) has odd perimeter. Mark the marking site adjacent to the unique green half-edge of the $\{G, B\}$-path of $S^*(\tau)$. The marking sites of (T, L) appear in a cyclic ordering on the boundary of the complement of T. Notice that performing two (G, B)-shears along the unique $\{G, B\}$-path of $S^*(\tau)$ moves the mark to the next marking site in the anti-clockwise order. This proves that the preimages of (T, L) form a single orbit under the horizontal shears and that the number of such preimages is the perimeter of (T, L).

Assume now that the perimeter is even, this corresponds to the case where the half-edges at the endpoints of the $\{G, B\}$-path of $S^*(\tau)$ have identical colours. Up to performing one (G, B)-shear (which has no effect on (T, L)), we can assume that both are green. We place two marks on (T, L), one next to each half-edge of the $\{G, B\}$-path of $S^*(\tau)$. These marks are *antipodal*: the number of marking sites between them on each side of the boundary of the complement of T is half the perimeter of (T, L). Like before, performing two (G, B)-shears along the unique $\{G, B\}$-path of $S^*(\tau)$ moves both marks to the next marking site in the anti-clockwise order. Since all the markings corresponding to a preimage with two green half-edges are antipodal, this proves that these the preimages are in a single orbit under the horizontal shears. Moreover, the number of such preimages is the half perimeter of (T, L). The same is true for preimages with two blue half-edges, and one alternates between one case and the other with each (G, B)-shear. □

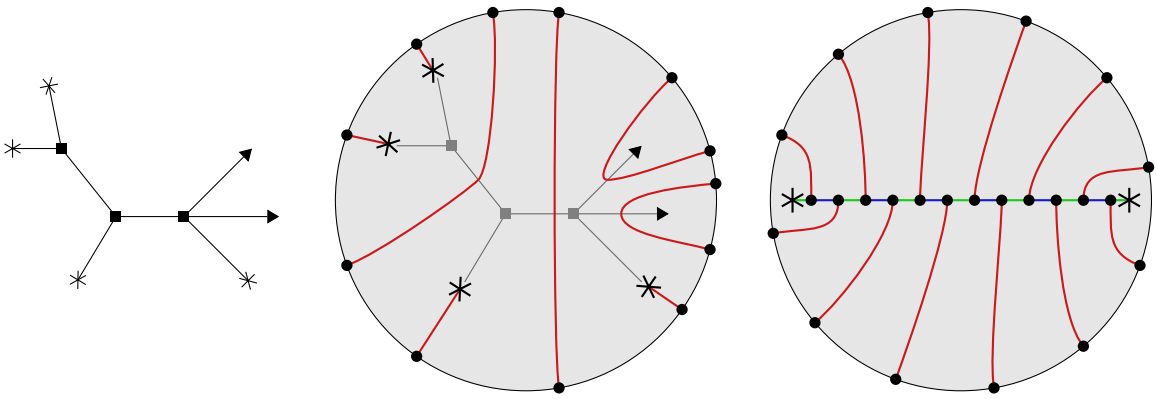

Figure 10: A decorated plane tree (T, L) with profile $([4, 3^2, 1^2], 4)$, its dual arch configuration and a $\{G, B\}$ path in a disk with same diameter. When drawing a decorated plane tree, we will represent the L-leaves by a star, and the other leaves by triangular nodes.

Theorem 3.1 directly follows from Theorem 3.2 and the following lemma.

Lemma 3.3. *Let (μ, k) be a spherical profile with $k \geqslant 2$. Then there exists a decorated plane tree with profile $(\mu, k-2)$.*

Proof. It is a standard result that a tree on n vertices with a given degree sequence $d_1, d_2, \ldots, d_n$ exists if and only if $d_1 + d_2 + \ldots + d_n = 2(n-1)$. Now for a tree with profile $(\mu, k-2)$ the number of vertices is $n = \sum \mu_i + k - 2$ and the degree sequence is $d = [1^{\mu_1+k-2}, 2^{\mu_2}, \ldots]$. The

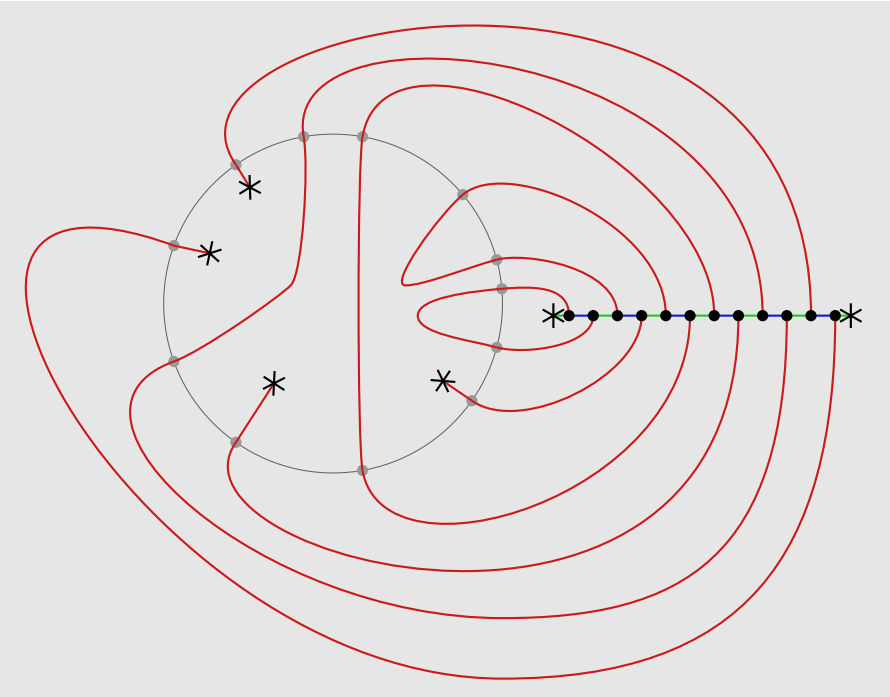

Figure 11: Matching the arch configuration and the $\{G, B\}$-path of Figure 10 to reconstruct a tricolored cubic graph as in the proof of Theorem 3.2.

planarity condition can be rewritten as

$$\sum_{i=1}^{n} d_i = k - 2 + \sum i\mu_i = 2\sum \mu_i + 2k - 6 = 2(n-1).$$

Thus there exists a tree with degree sequence d. In order to build a decorated plane tree, one just needs to pick any planar embedding and choose a subset of $k-2$ leaves. □

Note that the proof of Theorem 3.2 also provides a way of counting the number of path-like configurations in a stratum. For each decorated plane tree (T, L) in the stratum, the number of preimages, up to automorphism, is equal to the perimeter of (T, L) divided by its number of automorphisms.

Finally, the following proposition is an immediate consequence of the existence of path-like configurations and implies the lower bound in Theorem 1.7.

Proposition 3.4. *Let (μ, k) be a spherical profile, with $k \geqslant 2$. Then there are square-tiled surfaces with profile (μ, k) that are separated by $\Omega(k)$ cylinder shears.*

Proof. A shear can only change by at most two the number of half-edges coloured red in $S^*(\tau)$. By Theorem 3.1, there is a path-like square tiled-surface τ of profile (μ, k) and by symmetry, there is also a square tiled-surface τ' of profile (μ, k) that has a single vertical cylinder which furthermore is a path. Since τ and τ' have respectively $k-2$ and at most two red half-edges, this concludes the proof. □

3.2 Connecting to a path-like configuration

We now state and prove a general result about the reduction to path-like configurations of spherical square-tiled surface (see Lemma 3.5 below). Let us emphasise that it requires an

assumption on the profile that is not satisfied in general by spherical square-tiled surfaces, namely $\mu_1 \leqslant 1$. It is a partial step towards Theorem 1.7.

Lemma 3.5. *Let τ be a spherical square-tiled surface with profile (μ, k), such that $\mu_1 \leqslant 1$. Then τ can be connected to a path-like square-tiled surface τ' with a sequence of $O(k)$ vertical cylinder shears and powers of horizontal cylinder shears.*

The main technique to transform a spherical square-tiled surface into a path-like configuration is the fusion that we introduce now. Let τ be a square-tiled surface. A *fusion path* in τ is a vertical (or $\{R, G\}$) component of $S^*(\tau)$ that is a path and such that

- its intersection with each horizontal (or $\{G, B\}$) cycle is either empty or a single green edge,
- its intersection with each horizontal (or $\{G, B\}$) path is either empty or a single green half-edge.

Note that by definition a fusion path intersects at most two horizontal paths.

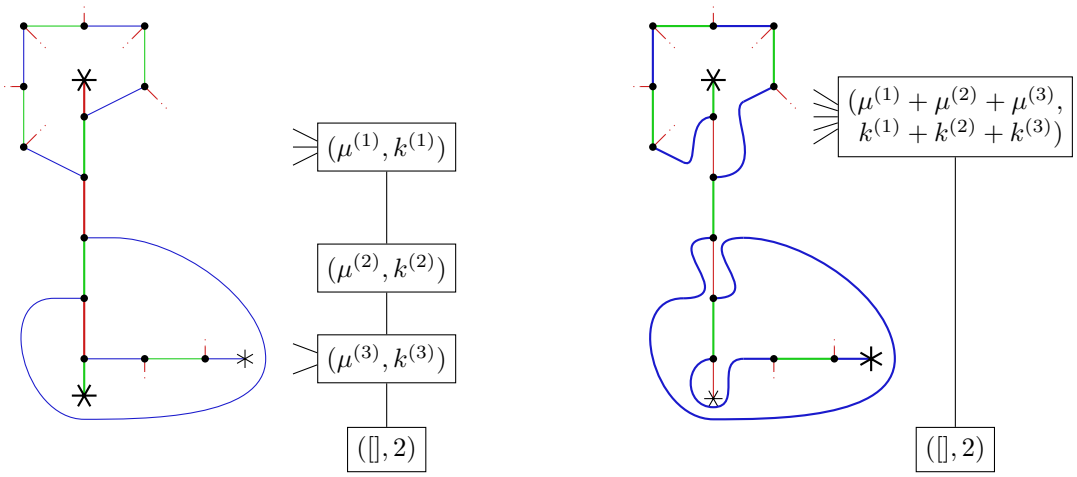

(a) A fusion path that intersects three $\{G, B\}$-components (two cycles and a path).

(b) The tricoloured cubic graph $S^*(\mathrm{Shear}_{c,R,G}(\tau))$.

Figure 12: A vertical shear on a fusion path results in merging the horizontal cylinders it crosses. To the right of each square-tiled surface τ and $\mathrm{Shear}_{c,R,G}(\tau)$ we draw the corresponding part of the stable graphs $\Gamma(\tau)$ and $\Gamma(\mathrm{Shear}_{c,R,G}(\tau))$.

Lemma 3.6. *Let τ be a square-tiled surface with n triangles and c be a fusion path in τ. Let U be the subset of $[n]$ that consists of the elements which belong to the vertical cylinders of τ which intersect c. Then in the square-tiled surfaces $\mathrm{Shear}_{c,R,G}(\tau)$ and $\mathrm{Shear}_{c,G,R}(\tau)$ the vertices of U form a single $\{G, B\}$-component (see Figure 12b).*

Let us note that Lemma 3.6 does not require planarity.

Proof. Let τ be a square-tiled surface and c a fusion path. We prove the case $\mathrm{Shear}_{c,R,G}(\tau)$, the case of $\mathrm{Shear}_{c,G,R}(\tau)$ being similar.

By relabelling τ, we assume that the vertices of c are labelled $1, 2, \ldots, m$ in such way that $\tau_R(i)$ and $\tau_G(i)$ belong to $\{i-1, i, i+1\}$. In particular, the two half-edges at the endpoints of c are adjacent to 1 and m.

Each horizontal (or $\{G, B\}$) cycle that intersects c does it along an edge with vertices i and $\tau_G(i) = i + 1$. We let H denote the ordered list of vertices on the $\{G, B\}$-cycle starting at $\tau_G(i)$ and ending at i. We let H' denote the same list where the first and last elements $\tau_G(i)$ and i have been exchanged.

Let s be the number of $\{G, B\}$-cycles intersecting the fusion path c (we have $m-2 \leqslant 2s \leqslant m$). We label these cycles from 1 to s according to the ordering of the vertices of c induced by our choice of vertex labelling of c and denote H_1, H_2, …, H_s their associated ordered lists.

If the vertex 1 in c is adjacent to a green half-edge, then we denote P_1 the list of vertices of the $\{G, B\}$-path containing 1 so that it ends with 1. If not, we let P_1 be the empty list. If the vertex m in c is adjacent to a green half-edge, then we denote P_m the list of vertices of the $\{G, B\}$-path containing m so that it starts with m. If not, we let P_m be the empty list.

The set U is the disjoint union of the elements in P_1, P_m, $H_1, \ldots, H_m$. After a (R, G)-shear in c, the $\{G, B\}$-path becomes the concatenation (in that order) of $P_1 \cdot H'_1 \cdot H'_2 \cdots H'_s \cdot P_m$. □

Let us recall that in Subsection 2.4, we introduced the weighted stable graph $\Gamma(\tau)$ associated to a square-tiled surface τ. Let us note that τ is path-like if and only if $\Gamma(\tau)$ is a graph made of two vertices, one of them having decoration $([], 2)$ and a unique edge between these two vertices that carries the decoration $(2n, \frac{1}{2})$.

We now reformulate Lemma 3.6 in terms of the weighted stable graph $\Gamma(\tau)$.

Lemma 3.7. *Let τ be a spherical square-tiled surface and let c be a fusion path in τ. In $S^*(\tau)$, each green edge of c belongs to a unique $\{G, B\}$-cycle and each green half-edge of c to a unique $\{G, B\}$-path. These $\{G, B\}$-components form a path c' in $\Gamma(\tau)$ that starts and ends at vertices with decorations $(\mu^{(start)}, k^{(start)})$ and $(\mu^{(end)}, k^{(end)})$ such that $k^{(start)} > 0$ and $k^{(end)} > 0$.*

Let $\tau' = \mathrm{Shear}_{c,R,G}(\tau)$. Then $\Gamma(\tau')$ is obtained from $\Gamma(\tau)$ by replacing all vertices in c' with two vertices u and v with decorations $(\mu^{(u)}, k^{(u)}) = ([], 2)$ and $(\mu^{(v)}, k^{(v)}) = \sum_{i \in c'} (\mu^i, k^i) - ([], 2)$ connected by a single edge and all neighbours of vertices in c in $\Gamma(\tau)$ get plugged to v.

Proof. The trace of c in $\Gamma(\tau)$ is a sequence of adjacent edges that do not repeat. Because $\Gamma(\tau)$ is a tree, this sequence of edges is an induced path. By definition of a fusion path, each endpoint of c is either a red half-edge or a green half-edge. In both cases, the associated vertex in $\Gamma(\tau)$ has a signature with a positive number k of half-edges.

The operation of fusion on $\Gamma(\tau)$ can be directly read from the description in Lemma 3.6. □

Finally, we state a lemma that allows us to find fusion paths in spherical square-tiled surfaces. It is a bit more general than what will be used to prove Lemma 3.5.

Lemma 3.8. *Let τ be a spherical square-tiled surface made of n triangles. Let $\Gamma(\tau)$ be the associated weighted stable tree. We assume that for each leaf $v \in V(\Gamma)$ the associated partition $(\mu^{(v)}, k^{(v)})$ satisfies $k^{(v)} \geqslant 1$. Let $i \in [n]$ such that it is either adjacent to a red half-edge in τ (i.e. $\tau_R(i) = i$) or such that i and its red neighbour $\tau_R(i)$ belong to distinct horizontal (or $\{G, B\}$) components. Then, there exists a square-tiled surface τ' obtained from τ by doing powers of horizontal cylinder shears such that the vertical component in τ' containing the image of this red edge or half-edge is a fusion path intersecting horizontal components. Furthermore, τ' can be chosen so that this fusion path ends at a leaf of the weighted stable tree $\Gamma(\tau) = \Gamma(\tau')$. Moreover, the number of powers of horizontal cylinder shears performed to obtained τ' from τ is at most the number of vertices in the image of the resulting fusion path in $\Gamma(\tau')$*

Proof. Let us first consider the case of i being adjacent to a red half-edge, that is $i = \tau_R(i)$. We denote e_0 this red half-edge and our aim is to extend it to a fusion path. If the horizontal (or $\{G, B\}$) component of $S^*(\tau)$ containing i is a path, then one can perform a power of a

horizontal cylinder shear on this path until e_0 becomes adjacent to a green half-edge. This $\{R, G\}$-path (made of two half-edges) is a fusion path. Let us assume now that i belongs to a $\{G, B\}$-cycle of $S^*(\tau)$ that we denote h_1. By the Jordan Curve theorem, h_1 separates the sphere into two distinct connected components. If the connected component that does not contain e_0 is a terminal component, i.e. a leaf of $\Gamma(\tau)$, then it contains a red half-edge e_1. Indeed, by assumption we have that $k^{(v)} > 0$ for every leaf $v \in \Gamma(\tau)$. In that case, one can apply a power of a horizontal cylinder shear on h_1 so that e_0 and e_1 become adjacent to a common green edge of h_1. This terminates the construction in that situation. Now, if the connected component is not a leaf of $\Gamma(\tau)$ then there exists a red edge e_1 in that connected component connecting h_1 to a distinct $\{G, B\}$-component h_2. By performing a horizontal cylinder shear on h_1 one can make e_0 and e_1 adjacent to a common green edge. We can continue this construction starting from e_1 instead of e_0 and obtain a fusion path.

To handle the case of $i \neq \tau_R(i)$, we cut this red edge into two half-edges e_0 and e_0' (the constructed square-tiled surface remains planar). The previous situation allows to build two fusion paths containing these two half-edges in some square-tiled surface τ'. Because τ' was obtained by performing only horizontal cylinder shears, e_0 and e_0' belong to the same face of τ' and we can glue them back and obtain a fusion path in some square-tiled surface τ''. It is easy to see that τ'' is obtained from τ.

Note that at most one power of a horizontal cylinder shear was performed for each horizontal component intersecting the fusion path. We claim that it is enough to do one such power in each horizontal cylinder of $S(\tau)$. Indeed, if two horizontal components of the cubic graph $S^*(\tau)$ belong to the same cylinder of $S(\tau)$ then performing a cylinder shear on one or the other results in isomorphic square-tiled surfaces. This concludes the proof. □

We are now ready to prove Lemma 3.5.

Proof of Lemma 3.5. Let $S(\tau)$ be a spherical square-tiled surface with profile (μ, k) with $\mu_1 \leqslant 1$. By Euler characteristic consideration, for each leaf v of the stable tree $\Gamma(\tau)$ we have $k^{(v)} + \mu_1^{(v)} \geqslant 2$. The assumption on μ_1 hence implies that $k^{(v)} \geqslant 1$ for each leaf v. In particular, τ satisfies the assumptions of Lemma 3.8.

Assume that τ is not path-like. Then there is a red edge in $S^*(\tau)$ whose endpoints belong to two distinct $\{G, B\}$-components. By Lemma 3.8, there exists a square-tiled surface τ' obtained from τ by a sequence of horizontal cylinder shears so that this red edge is part of a fusion path that ends in leaves of $\Gamma(\tau)$. By Lemma 3.7 performing a single vertical cylinder shear on this fusion path results in a square-tiled surface τ'' whose weighted stable graph $\Gamma(\tau'')$. One can continue this process until it reaches a path-like square-tiled surface.

Let us now count how many cylinder shears are performed. Each step involves some power of horizontal cylinder shears and a single vertical cylinder shear. We first derive a bound on the number of steps performed. Each step reduces the weighted stable graph by contracting a path between two leaves. The number of steps is hence bounded by the number of leaves, which is $O(k)$ (because each leaf of $\Gamma(\tau)$ corresponds to a component containing a half-edge). In particular, this bounds the number of vertical cylinder shears by $O(k)$. Let us now bound the number of powers of horizontal cylinder shears. At each step, this number is bounded by the length of the image of the fusion path in $\Gamma(\tau)$ used at that step. But since the fusion paths from different steps pass through different edges of the weighted stable graph their total number is at most the number of edges in $\Gamma(\tau)$ which also is $O(k)$. □

4 Reconfiguring path-like configurations

We now show that any two path-like configurations can be reconfigured efficiently into one another. Namely we prove the following.

Proposition 4.1. *Let (μ, k) be a spherical profile with $\mu_1 \leqslant 1$. Then any pair of path-like square-tiled surfaces τ and τ' in $\mathrm{ST}_{quad}(\mu)$ can be connected with a sequence of $O(k)$ powers of cylinder shears.*

Note that a closer look at the proof shows that this sequence uses *powers* of vertical cylinder shears instead of vertical cylinder shears only in the strata of the form $([1, 2^{\mu_2}, 3], 4)$.

Throughout this section, all the square-tiled surfaces we consider will be spherical and path-like. Using Theorem 3.2, we work directly on decorated plane trees on which we will define reconfiguration operations called *glue and cut* (see Subsection 4.1) and *decoration exchange* (see Subsection 4.2).

To show that two decorated plane trees are equivalent, a common technique in reconfiguration consists in showing that all decorated plane trees are equivalent to a specific one. The sketch of the proof is as follows. First, we show that all decorated plane trees are equivalent to some *nice* decorated plane tree: a decorated plane tree (T, L) with at most one $\overline{L}$-leaf and when it exists, this leaf is attached to a vertex of maximal degree (see Subsection 4.3). Second, we show that all nice decorated plane trees are equivalent up to a sequence of glue and cut operations to some nice decorated plane tree (T, L) with the additional property that T is a caterpillar, i.e. a tree whose internal vertices form a path (see Subsection 4.4). Finally, we show that all nice decorated plane caterpillars are equivalent by reordering the vertices of degree at least three (see Subsection 4.4). Using these intermediate lemmas, we conclude the proofs of Proposition 4.1 and Theorem 1.7 in Subsection 4.5.

4.1 Glue and cut

Let us recall from Subsection 3.1 that path-like configurations are square-tiled surfaces that admit a single $\{G, B\}$-component which furthermore is a path. To a path-like configuration one associates a decorated plane tree (T, L) which encodes its orbit under the unique $\{G, B\}$ cylinder shear, see Theorem 3.2.

The glue and cut operation on a decorated plane tree (T, L) is a reconfiguration operation that produces a new decorated plane tree (T', L'). It is better described decomposed in two steps. First, we delete two L-leaves and replace them by an edge between their parents. Then we delete an edge uv in the newly formed cycle and replace it by two pending L'-leaves attached to u and v (see Figure 13). The resulting decorated plane tree is (T', L'). Note that $|L| = |L'|$.

The following lemma shows that glue and cut operations on decorated plane trees decompose as a sequence of cylinder shears on the underlying square-tiled surfaces.

Lemma 4.2. *Let τ_1 and τ_2 be the two path-like square-tiled surfaces with associated decorated plane trees (T_1, L_1) and (T_2, L_2) that differ by one glue and cut operation. Then τ_1 can be connected to τ_2 with a sequence of shears made of at most two vertical shears and four powers of horizontal shears.*

Proof. The reconfiguration sequence is illustrated by an example in Figure 13.

Recall that L_1 is the subset of leaves of T_1 which are dual to red half-edges in τ_1. Let a_1 and b_1 denote the elements of L_1 that are joined by the glue operation. Let also e_1 denote the edge of T_1 removed by the cut operation.

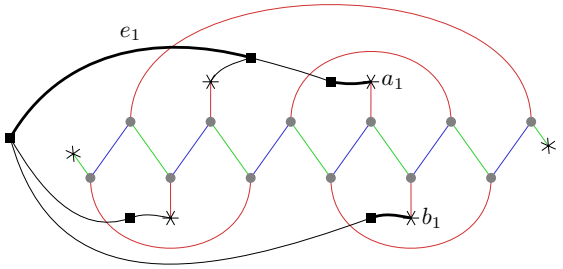

(a) Up to a power of a horizontal shear, the two half-edges a_1 and b_1 impacted by the gluing are incident to a common green edge.

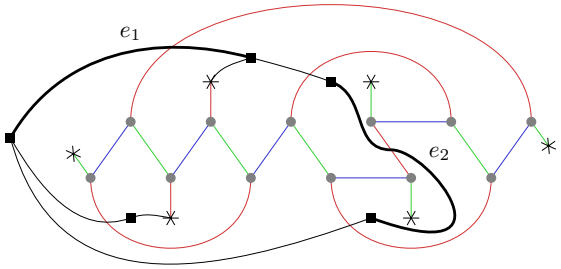

(b) The configuration obtained from Figure 13a after the vertical shear on the $\{R, G\}$-path connecting the dual of a_1 and b_1.

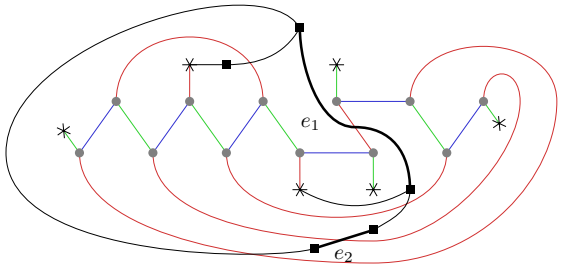

(c) The configuration obtained from Figure 13b after powers of horizontal shears on its two $\{G, B\}$-paths.

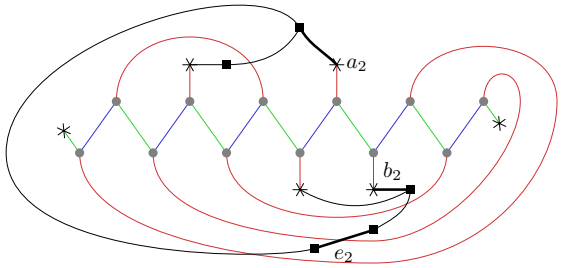

(d) The configuration obtained from Figure 13c after the vertical shear on the $\{R, G\}$-path containing the dual of e_1.

Figure 13: Glue and cut operation. The outer face is marked by a square node. The edges and leaves impacted by the glue and cut operation are thickened.

First, perform in τ_1 a power of the horizontal shear on the unique $\{G, B\}$-path until the dual half-edges of a_1 and b_1 are at distance 3 in the tricoloured cubic graph $S^*(\tau)$ and separated by a green edge (see Figure 13a). Then, performing a vertical shear on the path between the dual half-edges to a and b breaks the $\{G, B\}$-path into two $\{G, B\}$-paths P and Q (see Figure 13b). After this operation, the tricoloured cubic graph is not path-like anymore and the dual of the red edges is a graph that consists of the tree T_1 in which a_1 and b_1 have been joined to form an edge (see Figure 13b). We call e_2 the edge in this graph resulting from the fusion of a_1 and b_1. Note that the edge e_1 still exists in this graph and is distinct from e_2.

Next, by performing a power of a horizontal shear on each of the $\{G, B\}$-paths P and Q, we move the red edge dual to e_1 such that it connects the endpoints of P and Q and that there is a green half-edge adjacent at each of these endpoints (see Figure 13c). The choice of which endpoints of P and Q are used at this step is irrelevant. Next, we perform a vertical shear on the $\{R, G\}$-path containing the red edge dual to e_1. This operation destroys e_1 in the graph dual to the red edges and creates instead to leaves a_2 and b_2. The two paths P and Q of the tricoloured cubic graph are merged into a single $\{G, B\}$-path, thereby obtaining a path-like configuration again (see Figure 13d). By construction, the decorated plane tree associated to this resulting tricoloured cubic graph is (T_2, L_2). Finally, by Theorem 3.2 we can use one more power of a $\{G, B\}$-shear along the unique $\{G, B\}$-path to reach τ_2.

The sequence of cylinder shears constructed above from τ_1 to τ_2 provides the bound from the statement and concludes the proof. □

4.2 Decoration exchange

In this subsection, we present another reconfiguration operation on decorated plane trees called *decoration exchange*, that given a decorated plane tree (T, L), modifies L but not T. Similarly to the glue and cut operation from Subsection 4.1 we prove that this operation on decorated plane trees can also be obtained by a sequence of cylinder shears on the underlying square-tiled surfaces.

Let (T, L) be a decorated plane tree containing the two following subtrees: a $\overline{L}$-leaf u, and two L-leaves v, w adjacent to a common vertex x and consecutive in the cyclic ordering of the vertices around x. Let L' be the set of leaves of T obtained by replacing v by u in L. We say that (T, L) and (T, L') differ by a *decoration exchange*.

The operation is illustrated in Figure 14.

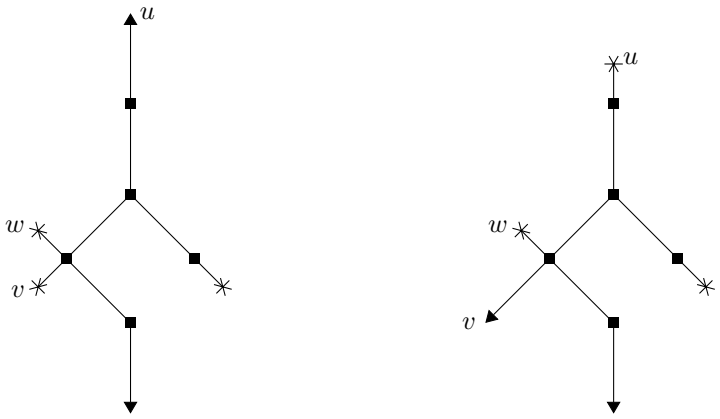

Figure 14: A decoration exchange on decorated plane trees.

Lemma 4.3. *Let (T, L) and (T, L') be two decorated plane trees that differ by a decoration exchange. Let τ and τ' be two path-like configurations whose decorated plane trees are respectively (T, L) and (T, L') respectively. Then τ can be connected to τ' by a sequence made of at most two vertical cylinder shear and 4 powers of horizontal shears.*

Proof. Figure 15 shows an illustrative example of the tricoloured cubic graphs in the reconfiguration sequence.

Recall that on a decorated plane tree (T, L) associated to a path-like configuration τ, the $\overline{L}$-leaves correspond to the 1-faces of the tricoloured cubic graph $S^*(\tau)$, which are geometrically triangles. Equivalently, they correspond to vertices of degree 3 in the square-tiled surface $S(\tau)$.

Let u be the $\overline{L}$-leaf of T and v, w the two L-leaves impacted by the decoration exchange. Let x be the common neighbour of v and w. Perform in $S^*(\tau)$ a power of the horizontal shear on the unique $\{G, B\}$-path until the half-edge dual to w is adjacent to the face of degree 3 dual to u (see Figure 15a). Perform a vertical shear on the $\{R, G\}$-path composed of the half-edges dual to v and w and passing by the face of degree 3 dual to u. This separates the $\{G, B\}$-path into two $\{G, B\}$-paths P and Q, adds v to L and replaces u and w by an edge e in the decorated plane tree (see Figures 15b and 15c). Perform on P and Q a power of a horizontal shear, until the edge dual to e connects the extremities of both paths (see Figure 15d). Perform a vertical shear on the edge dual to e and the incident green half-edges. This replaces e by two leaves u and w of L' and yields the desired decorated plane tree (T, L').

Finally, by Theorem 3.2 we can use one more power of a $\{G, B\}$-shear along the unique $\{G, B\}$-path to reach τ'. □

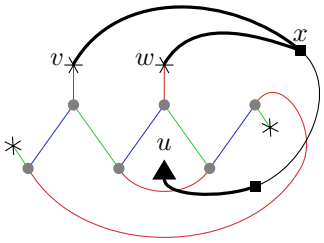

(a) Up to a power of a horizontal shear, the half-edge corresponding to w is adjacent to the 1-face in the initial configuration

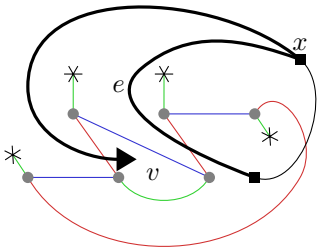

(b) After a vertical shear, the 1-face is moved and two half-edges are merged into an edge e

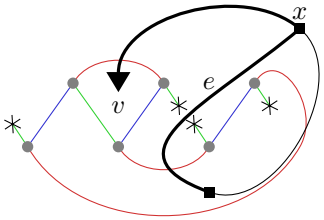

(c) Same configuration as Figure 15b

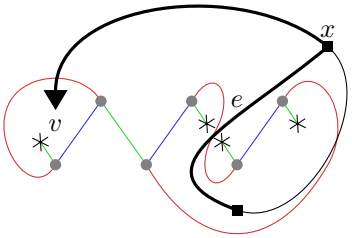

(d) After a power of a horizontal shear, the edge e connect the extremities of the two $\{G, B\}$-paths P_1, P_2

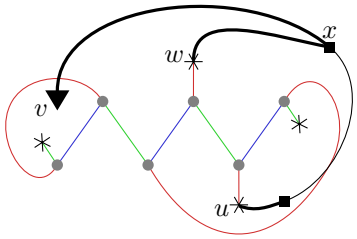

(e) After a vertical shear on e and the incident red half-edges, e is replaced by two L'-leaves

Figure 15: How to realise a decoration exchange with a sequence of cylinder shears

4.3 Making a decorated plane tree nice

In this section we describe how the glue and cut operation and the decoration exchange operation can be combined to transform any decorated plane tree into a nice tree.

Recall the following definition: A decorated plane tree (T, L) of profile $(\mu, k-2)$ is *nice* if $\mu_1 = 0$ or if $\mu_1 = 1$ and the only $\overline{L}$-leaf of T is adjacent to a vertex of maximal degree.

The following technical lemmas connect decorated plane trees to nice ones, but only in the subset of spherical profiles with $\mu_1 \leqslant 1$. Lemma 4.4 handles all such profiles but those of the form $([1, 2^{\mu_2}, 3], 4)$, which are handled by Lemma 4.5.

Lemma 4.4. *Let (T, L) be a decorated plane tree of profile $(\mu, k-2)$, such that $\sum \mu_i(i-2) = k-4$, with $\mu_1 \leqslant 1$ and $(\mu, k) \neq ([1, 2^{\mu_2}, 3], 4)$. There exists a sequence composed of at most one decoration exchanges and two glue and cut operations that leads to a nice decorated plane tree of profile $(\mu, k-2)$.*

Proof. If $\mu_1 = 0$, then (T, L) is already nice. If $\mu_1 = 1$ and $k = 3$, then (T, L) is also nice

because T is a path. Finally, if $\mu_1 = 1$ and $k \geqslant 4$, then the assumption $(\mu, k) \neq ([1, 2^{\mu_2}, 3], 4)$ is equivalent to $k \geqslant 5$, that is $|L| \geqslant 3$. The reconfiguration sequence is illustrated by an example in Figure 16.

Let u be a vertex of T of maximal degree such that L intersects at least three connected components of $T \setminus u$. Such a vertex exists if T has maximum degree at least four, in which case any vertex of maximum degree satisfies this condition because there is only one $\overline{L}$-leaf of T. If T has maximum degree three, then it contains at least two vertices of vertices of degree three and at most one of them does not verify this condition.

Let t be the $\overline{L}$-leaf of T. Let v, w, x be three leaves of L in distinct connected components of $T - u$, such that the connected components containing v and w appear consecutively around u (see Figure 16a). Perform the glue and cut operation that replaces v and w by an edge and cuts one of the edges incident to u (see Figure 16a). One of the two leaves y, z created by this operation is adjacent to u, say y (see Figure 16b). Perform the glue and cut operation that replaces x and z by an edge and cuts the edge incident to u and consecutive to y (see Figure 16b). In the decorated plane tree (T_f, L_f) obtained after this operation (see Figure 16d), u is adjacent to two consecutive leaves of L_f and a decoration exchange on t and these leaves results in a nice decorated plane tree. □

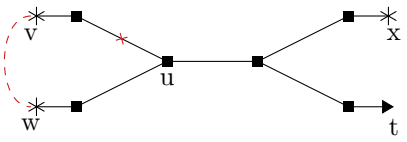

(a) Original decorated plane tree (T', L')

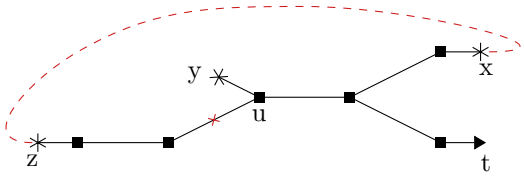

(b) Decorated Plane tree obtained after one glue and cut operation

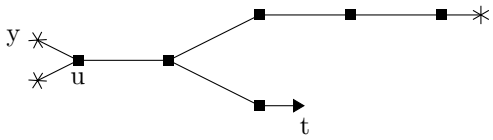

(c) Decorated Plane tree obtained after another glue and cut operation

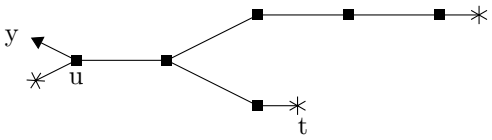

(d) The nice decorated plane tree (T_f, L_f) after a decoration exchange

Figure 16: Obtaining a nice decorated plane tree when $\mu_1 + k \geqslant 6$. The glue and cut operations resulting in the next subfigure are represented in red: the glued half-edges are connected by a dashed path and the cut edge is crossed.

Lemma 4.5. *Let τ be a path-like configuration with profile $(\mu, k) = ([1, 2^{\mu_2}, 3], 4)$. There exists a sequence composed of $O(1)$ powers of horizontal shears and powers of vertical shears that leads to path-like configuration corresponding to a nice decorated plane tree.*

Proof. The decorated plane tree (T, L) associated to τ has one vertex u of degree three, μ_2 vertices of degree two, and three leaves, two of them belonging to L. After one glue and cut operation, we obtain a decorated plane tree (T', L') in which an L'-leaf is adjacent to u. Let t be the $\overline{L}'$-leaf and m be number of vertices of degree two on the path between u and t. Note that (T', L') is nice if and only if $m = 0$, thus our goal is to reduce m.

Let τ' be some path-like configuration corresponding to (T', L'). By Lemma 4.2, τ and τ' differ by $O(1)$ vertical shears and powers of horizontal shears. Label the vertices of $S^*(\tau')$ in the order on which they appear on the unique $\{G, B\}$-path. Up to performing a power of the horizontal shear, one can assume that $\tau'_R(1) = 3$, i.e. the only 1-face in $S^*(\tau')$ contains

no half-edges in its border but is adjacent to a green half-edge via the vertex labelled 1 (see Figures 17a and 18a).

Thus, $(1, 2, 3, \dots 2m+2, 2m+3, \dots 2\mu_2+2)$ is the unique $\{G, B\}$-path in $S^*(\tau')$ and $P = (1, 3, 2, 5, 4, \dots 2i+3, 2i+2, \dots 2m+3, 2m+2)$ is a $\{R, G\}$-path in $S^*(\tau')$.

We claim that after performing m $\{R, G\}$-shears on P, we obtain a path-like configuration τ'', whose $\{G, B\}$-path is the following sequence. If m is even (see Figure 17b), then the $\{G, B\}$-path is:

$$(2\mu_2+2, \dots 2m+4, m+3, m+2, \underbrace{(m+1-i, m+2-i, m+4+i, m+3+i)}_{\text{for } 1 \leqslant i \leqslant m/2}, 1)$$

If m is odd (see Figure 18b), then the $\{G, B\}$-path is:

$$(2\mu_2+2, \dots 2m+4, \underbrace{(m+i, m+3+i, m+3-i, m-i)}_{\text{for } 1 \leqslant i \leqslant (m-1)/2}, 2m, 2m+3, 3, 1, 2m+2)$$

Each case can be easily checked by an induction on $\lfloor m/2 \rfloor$, the key argument being that the order in which the vertices $1, \dots 2m+3$ are visited by the $\{G, B\}$-path of $S^*(\tau'')$ is monotone with respect to the distance to the middle of the $\{R, G\}$-path P. The 1-face of $S^*(\tau'')$, induced by the vertices $\{m, m+2, m+3\}$ if m is even, respectively by $\{m+1, m+2, m+4\}$ if m is odd, is adjacent to the 3-face of $S^*(\tau'')$ via the red edge $(m\, m+3)$, respectively $(m+1\, m+2)$. In other words, t is adjacent to u in the nice decorated plane tree (T'', L'') associated to τ'', which concludes the proof. □

By combining Lemma 4.4 and Lemma 4.5 along with Lemma 4.3 and Lemma 4.2, we directly obtain the following.

Corollary 4.6. *Let τ be a spherical path-like configuration. There exists a sequence composed of $O(1)$ powers of horizontal shears and powers of vertical shears that leads to path-like configuration corresponding to a nice decorated plane tree.*

4.4 Equivalence of nice decorated plane trees

Let $\mu = [1^{\mu_1}, 2^{\mu_2}, 3^{\mu_3} \dots]$ and $k = \sum_i \mu_i(i-2)+4$, such that $\mu_1 \leqslant 1$. To prove Theorem 1.7, we only need to prove that all nice decorated plane trees with the profile $(\mu, k-2)$ are equivalent up to a sequence of glue and cut operations.

We will proceed in two steps: first proving that any nice decorated plane tree is equivalent up to a sequence of glue and cut operations to a nice decorated plane tree (T, L) where T is a caterpillar, and then showing that all such decorated plane trees are equivalent up to a sequence of glue and cut operations.

Lemma 4.7. *Let (T, L) be a nice decorated plane tree of profile $(\mu, k-2)$. There exists a sequence of at most k glue and cut operations and that connects (T, L) to a nice decorated plane tree (T', L') with identical profile, where T' is a caterpillar.*

Proof. The assumption $\mu_1 \leqslant 1$ guarantees that there is at most one $\overline{L}$-leaf of T. Let P be a maximal path, containing the $\overline{L}$-leaf if it exists. Let a and b be the two leaves at the extremities of P (see Figure 19), without loss of generality, we assume that $a \in L$. We prove that if T is not a caterpillar, then we can increase the length of P by performing one glue and cut operation.

Let c be a leaf at distance at least 2 from P. Let Q be the path from a to c and uv be the last edge of Q belonging to P. Perform the glue and cut operation that replaces the leaves a and c by an edge e and that removes the edge uv. It results in a longer path going from b to v via P, then to e via Q and finally to u via P. □

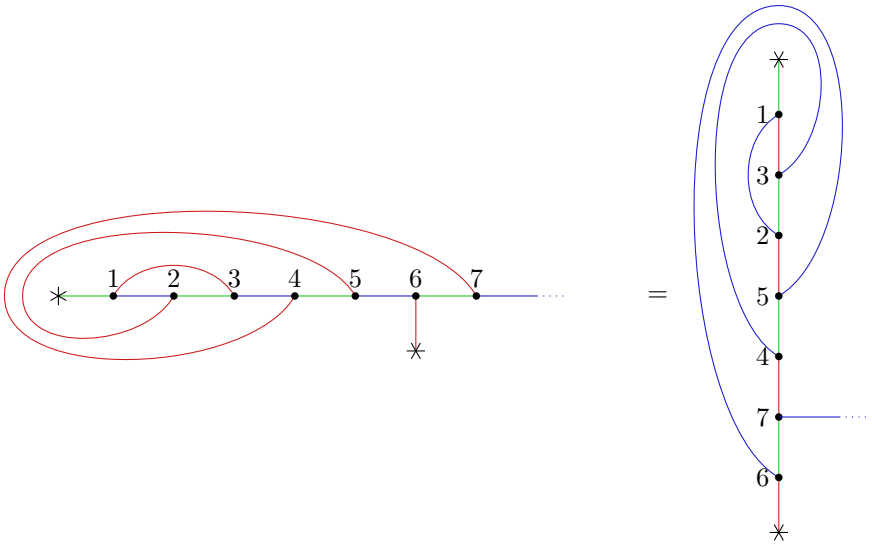

(a) $S^*(\tau')$ is path-like and contains the $\{R, G\}$-path $1, 3, 2, 5, 4, \dots 2i+3, 2i+2, \dots 2m+3, 2m+2$.

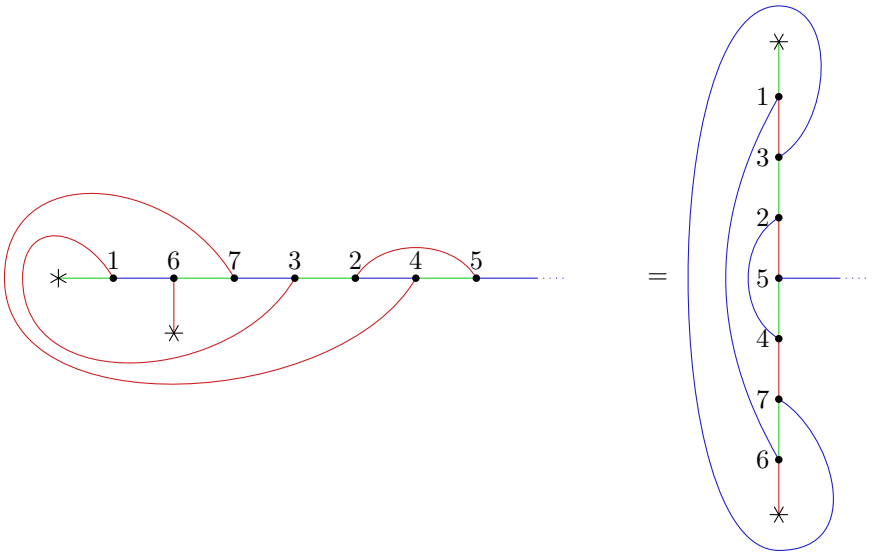

(b) After m $\{R, G\}$-shears, $S^*(\tau'')$ is still path-like and corresponds to a nice decorated plane tree

Figure 17: Obtaining a nice decorated plane tree when $(\mu, k) = ([1, 2^{\mu_2}, 3], 4)$. Even case, here m= 2.

We call *spine* of a caterpillar its internal vertices, in the order they appear on the path going from one extremity to the other. Let (T^*, L^*) be the nice decorated plane tree such that T^* is a caterpillar whose spine $(u_1, \dots u_n)$ is a sequence of non-increasing degree, in which all leaves adjacent to $u_2, \dots u_n$ belong to L^*. Note that this definition leaves out the ambiguity of the positions of the leaves around each vertex in the plane embedding of T^*. Hence, we further require all u_i to be *cyclically ordered*, that is that all the L^*-leaves around u_i appear after u_{i-1} (or u_2 for $i = 1$) and consecutively in the anti-clockwise order (see Figure 20).

Lemma 4.8. *Let (T, L) be a nice decorated plane tree with profile $(\mu, k-2)$, such that T is a caterpillar. There exists a sequence of $O(k)$ glue and cut operations and decoration exchanges leading from (T, L) to (T^*, L^*).*

Proof of Lemma 4.8. Let (T, L) be a nice decorated plane tree of profile $(\mu, k-2)$ with T a caterpillar and $(u_1, \dots u_n)$ its spine. If $k + \mu_1 = 4$, there is only one nice decorated plane tree

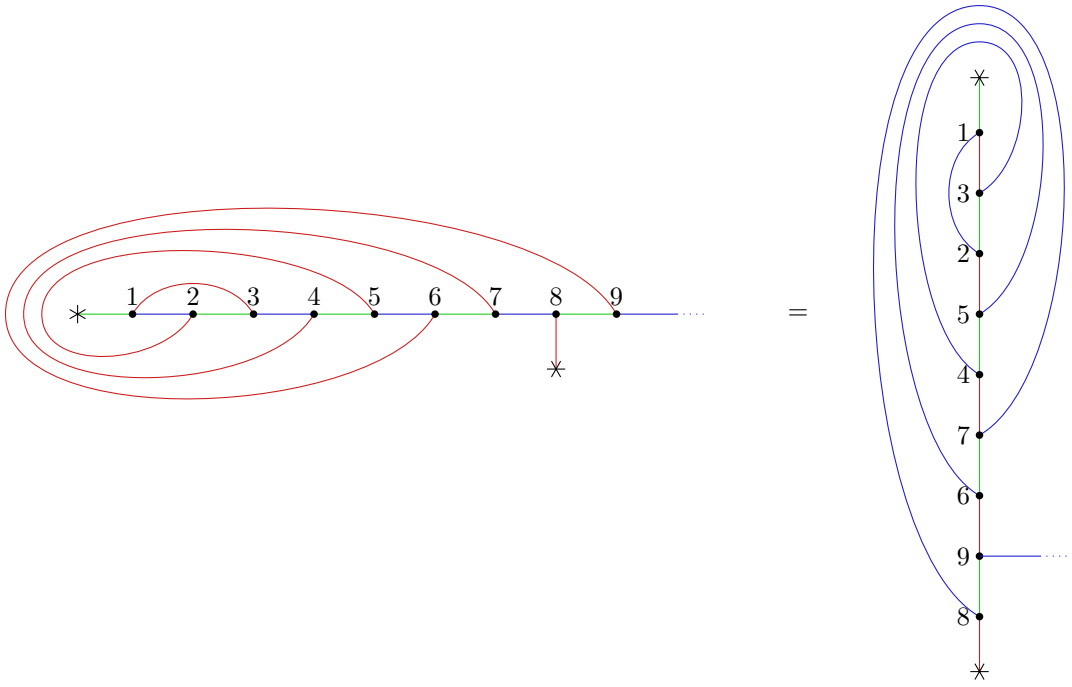

(a) $S^*(\tau')$ is path-like and contains the $\{R, G\}$-path $1, 3, 2, 5, 4, \dots 2i+3, 2i+2, \dots 2m+3, 2m+2$.

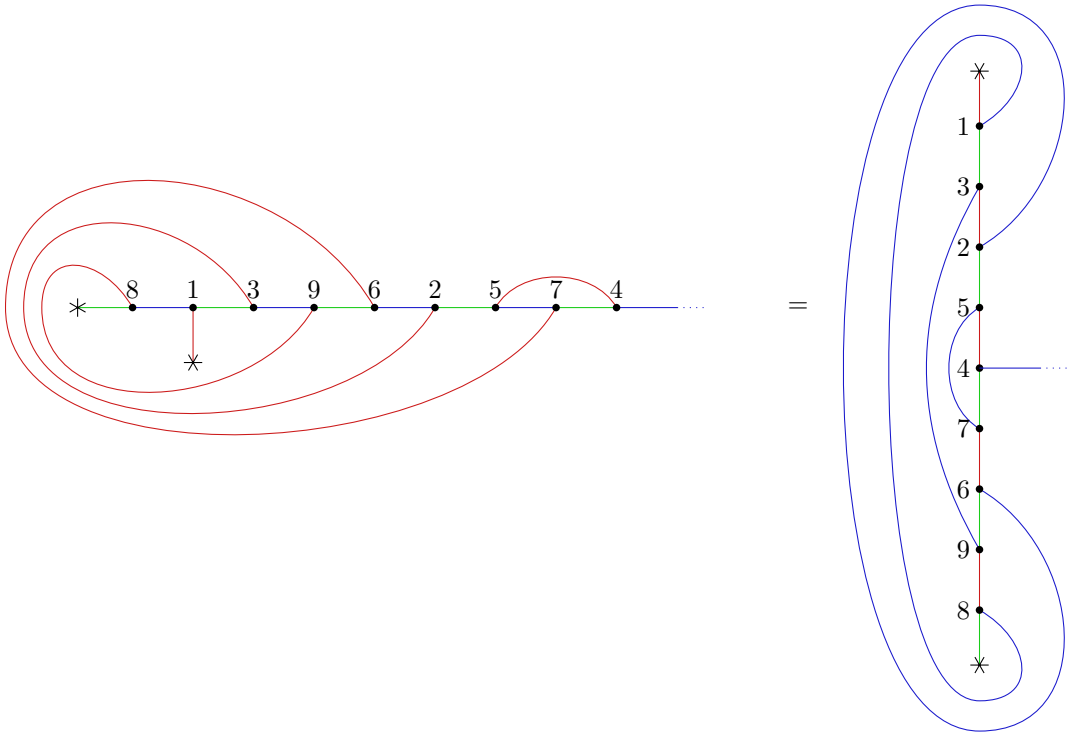

(b) After m $\{R, G\}$-shears, $S^*(\tau'')$ is still path-like and corresponds to a nice decorated plane tree

Figure 18: Obtaining a nice decorated plane tree when $(\mu, k) = ([1, 2^{\mu_2}, 3], 4)$. Odd case, here m= 3.

of profile $(\mu, k-2)$, so we are done. We now assume that $k + \mu_1 \geqslant 5$. We first prove a claim that allows us to perform some permutations of the spine. We will use it to sort the degree of the vertices on the spine and obtain (T^*, L^*).

Claim 4.9. *Assume that all u_1 is adjacent to at least two L-leaves. Let u_i be a vertex of the spine. By performing at most three glue and cut operations and at most two decoration exchanges,*

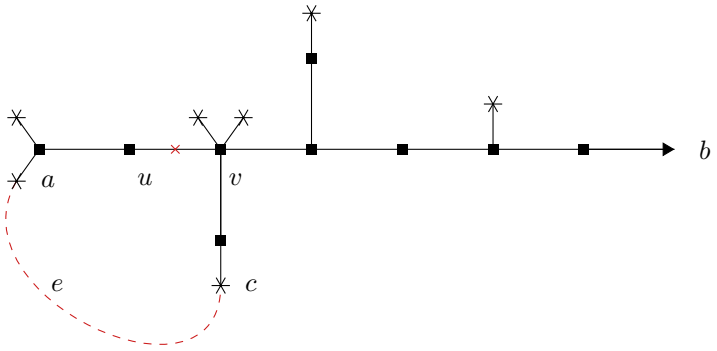

Figure 19: Extending the longest path of a decorated plane tree. The dashed edge represents the gluing of L-leaves while the edge that is cut is crossed.

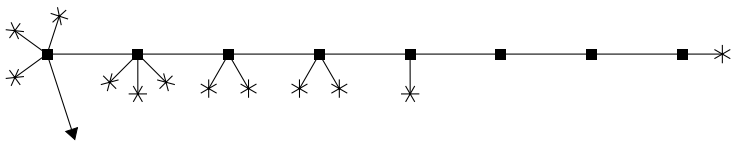

Figure 20: The nice decorated plane tree (T^*, L^*) for the profile $([1, 2^3, 3, 4^2, 5^2], 12)$

one can move u_i to obtain a nice decorated plane caterpillar (T', L') with spine $(u_i, u_1, \dots u_{i-1}, u_{i+1}, \dots u_n)$. Moreover, u_i is cyclically ordered in (T', L') and each other vertex u_j stays cyclically ordered if it was the case in (T, L) and all adjacent leaves in (T, L) belonged to L.

Proof. Let I be the set of indices for which u_j is cyclically ordered and has all its adjacent leaves in L. The procedure is illustrated by Figure 21.

Denote a and b the first and last L-leaves adjacent to u_1 in the anti-clockwise order after u_2. Note that if $1 \in I$, then all its adjacent L-leaves appear between a and b in the anti-clockwise order. Likewise, for all $j \in I \setminus \{1\}$, all leaves adjacent to u_j appear between u_{j-1} and u_{j+1} in the anti-clockwise order.

Note that u_n is adjacent to some L-leaf c: by assumption (T, L) is nice, so if $\deg(u_n) = 2 < \deg(u_1)$, u_n is adjacent to one L-leaf; and if $\deg(u_n) \geqslant 3$, then u_n is also adjacent to at least one L-leaf (see Figure 21a). Take c to be the first L-leaf after u_{n-1} in the clockwise order.

Perform the glue and cut operation that replaces the leaves b and c by an edge and that cuts the edge $u_{i-1}u_i$ to replace it by a leaf d adjacent to u_{i-1} and a leaf e adjacent to u_i (see Figure 21a). It produces a caterpillar with spine $(u_i, \dots u_n, u_1 \dots u_{i-1})$ (see Figure 21b). Perform a glue and cut operation that replaces the leaves a and e by an edge and that cuts the edge u_iu_{i+1} to replace it by a leaf f adjacent to u_i and a leaf g adjacent to u_{i+1} (see Figure 21b). It produces a tree that is not a caterpillar anymore, in which u_n and u_i are adjacent to u_1 (see Figure 21c). Finally, perform the glue and cut operation that replaces the leaves c and g by an edge and cuts the edge u_1u_n (see Figure 21c). It produces a caterpillar with the desired spine (see Figure 21d).

As it can be easily checked on Figure 21, all vetices u_j with $j \in I$ are still cyclically ordered. It is however possible that u_1 is not yet cyclically ordered if it is adjacent to the $\overline{L}$-leaf, in which

case u_1 is also adjacent to an L-leaf and two consecutive decoration exchanges with any other L-leaf can make u_1 cyclically ordered, as desired. □

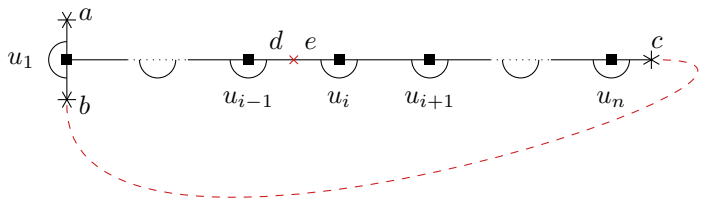

(a) Original caterpillar with spine $(u_1, \dots u_n)$ and u_1 adjacent to at least two L-leaves

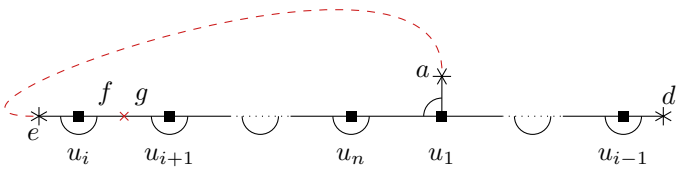

(b) After one glue and cut operation, the spine becomes $(u_i, u_{i+1} \dots u_n, u_1, \dots u_{i-1})$

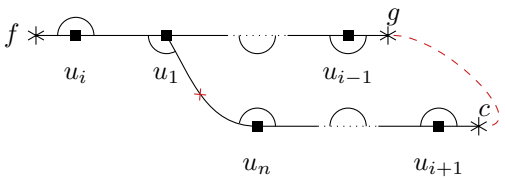

(c) After one more glue and cut operation, the decorated plane tree is not a caterpillar anymore

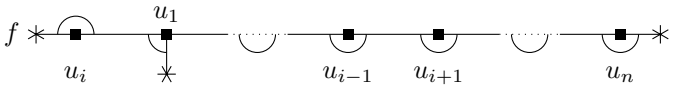

(d) Final caterpillar with spine $(u_i, u_1, \dots u_{i-1}, u_{i+1}, \dots u_n)$

Figure 21: Moving u_i to the front of the caterpillar. Again, the glue and cut operations resulting in the next subfigure are represented in red: the glued half-edges are connected by a dashed path and the cut edge is crossed. The arcs around the vertices represent the positions of the remaining L-leaves, for the vertices u_j with $j \in I$.

We first ensure that the one of the extremities of the spin is of degree at least three. If that is not the case, each extremity is adjacent to an L-leaf, say a and b respectively. Since $k + \mu_1 \geqslant 5$, there is a internal vertex u that is adjacent to an L-leaf. Perform the glue and cut operation that replaces a and b by an edge and cuts an edge incident to u. It produces a caterpillar in which u is adjacent to two L-leaves and is placed at one extremity of the spin.

Let $v_1, \dots v_p$ be all the vertices of degree at least three in T, ordered such that for all i, $\deg(v_i) \leqslant \deg(v_{i+1})$ and for all $i < p$, the leaves adjacent to v_i all belong to L.

We can apply Claim 4.9 successively to each of the v_i. This results in (T^*, L^*). The corresponding reconfiguration sequence has length $O(\sum_i \mu_i) = O(k)$ □

4.5 Proof of Proposition 4.1 and Theorem 1.7

Theorem 1.7 from the introduction follows directly from Lemma 3.5 that was proved in Section 3 and Proposition 4.1 that we prove now.

Proof of Proposition 4.1. Let τ be a path-like square-tiled spherical surface with profile (μ, k). By Corollary 4.6, τ is connected by a sequence of $O(1)$ powers of cylinder shears to a path-like square-tiled surface τ' that corresponds to a nice decorated plane tree (T', L').

Let (T^*, L^*) be the decorated plane tree of profile $(\mu, k-2)$ defined before Lemma 4.8. By Theorem 3.2, there is a path-like configuration τ^* with profile (μ, k) that maps to (T^*, L^*).

By Lemmas 4.7 and 4.8, (T', L') can be connected to (T^*, L^*) via $O(k)$ glue and cut operations and decoration exchanges. Hence, τ and τ^* are equivalent up to $O(k)$ powers of cylinder shears by Lemma 4.2 and Lemma 4.3. This is true for all path-like square-tiled surfaces in $ST_{quad}(\mu, k)$, which concludes the proof of Proposition 4.1. □

Combined with Lemma 3.5, this proves that any two spherical square-tiled surfaces of profile (μ, k) with $\mu_1 \leqslant 1$ are connected up to $O(k)$ powers of cylinder shears, thereby concluding the proof of Theorem 1.7.

5 Hyperelliptic square-tiled surfaces

This section focuses on the hyperelliptic Abelian components. We first give in Subsection 5.1 a more precise description of the quotient of such square-tiled surfaces by the hyperelliptic involution. Then in Subsection 5.2 we explain the effect of a cylinder shear on the quotient by the hyperelliptic involution. In Subsection 5.3 we show how hyperelliptic Abelian square-tiled surfaces can be connected to path-like configurations using cylinder shears. Finally, we conclude the proof of Theorem 1.6 in Subsection 5.4 by reducing to Theorem 1.7.

5.1 Hyperelliptic components

Following [KZ03] we define the subsets $\mathrm{ST}^{hyp}_{Ab}([2^{\mu_2}, (2g)^2])$ and $\mathrm{ST}^{hyp}_{Ab}([2^{\mu_2}, 4g-2])$ of respectively $\mathrm{ST}_{Ab}([2^{\mu_2}, (2g)^2])$ and $\mathrm{ST}_{Ab}([2^{\mu_2}, 4g-2])$ (recall from Subsection 1.3 that we use the notation $\mathrm{ST}(\mu)$ instead of $\mathrm{ST}(\mu, k)$ when $k = 0$, which is always the case for Abelian square-tiled surfaces). These subsets correspond to the square-tiled surfaces that belong to the so-called hyperelliptic components of the moduli space of Abelian differentials. By Proposition 1.5 proven at the end of Subsection 2.3, these subsets are invariant under cylinder shears. However, we propose in this subsection an alternative combinatorial proof.

Let $\tau = (\tau_R, \tau_G, \tau_B) \in (S_n)^3$ be a square-tiled surface in some stratum $\mathrm{ST}(\mu, k)$. An *automorphism* of τ is a permutation $\alpha \in S_n$ that normalises simultaneously τ_R, τ_G and τ_B that is : $\alpha\tau_i\alpha^{-1} = \tau_i$ for any colour $i \in \{R, G, B\}$. We denote $\mathrm{Aut}(\tau)$ the automorphism group of τ.

Let H be a subgroup of $\mathrm{Aut}(\tau)$. We define the quotient square-tiled surface $\tau' = \tau/H$ whose set of squares are the orbits of H on $[n]$ and $(\tau'_R, \tau'_G, \tau'_B)$ are the induced action on the orbits. Note that when taking the quotient, one needs to choose a labelling of the H-orbits in $[n]$ with $[n']$. A canonical choice consists in ordering these orbits according to the minimal element.

A square-tiled surface τ of genus $g \geqslant 2$ is *hyperelliptic* if it admits an automorphism α which is of order 2 and such that the quotient $\tau/\langle\alpha\rangle$ has genus 0.

Let $g \geqslant 2$ and $\mu_2 \geqslant 0$. We define $\mathrm{ST}^{hyp}_{Ab}([2^{\mu_2}, 4g-2])$ to be the subset of $\mathrm{ST}_{Ab}([2^{\mu_2}, 4g-2])$ that are hyperelliptic and $\mathrm{ST}^{hyp}_{Ab}([2^{\mu_2}, (2g)^2])$ to be the subset of $\mathrm{ST}_{Ab}([2^{\mu_2}, (2g)^2])$ that are

hyperelliptic and such that the hyperelliptic involution exchanges the two singularities of degree $2g$.

It is a standard result that a translation or half-translation surface of genus $g \geqslant 2$ admits at most one hyperelliptic involution. Furthermore, if it exists it is central in the automorphism group (i.e. all other automorphisms commute with the hyperelliptic involution). These two facts follow from the result that for a Riemann surface X, the induced action on homology gives rise to an injective map $\mathrm{Aut}(X) \to \mathrm{Sp}(H_1(X;\mathbb{Z}))$ and the image of the hyperelliptic involution is $-Id$, see [FM11, Theorem 6.8].

We warn the reader that for the profile $\mu = [2^{\mu_2}, (2g)^2]$ the condition that the hyperelliptic involution exchanges the two singularities of degree $2g$ is important. More precisely, there exists hyperelliptic square-tiled surfaces in $\mathrm{ST}_{Ab}([2^{\mu_2}, (2g)^2])$ whose quotient belongs to a spherical square-tiled surface in some strata $\mathrm{ST}_{quad}([1^{\mu'_1}, 2^{\mu'_2}, (g)^2], k)$, see Figure 22.

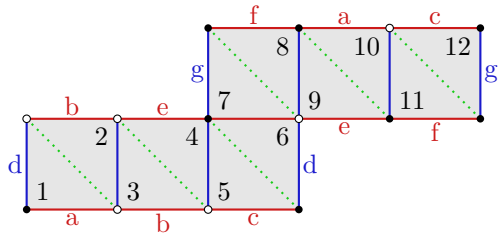

$\tau_R = (1,10)(3,2)(5,12)(7,6)(9,4)(11,8)$
$\tau_G = (1,2)(3,4)(5,6)(7,8)(9,10)(11,12)$
$\tau_B = (1,6)(3,2)(5,4)(7,12)(11,10)(9,8)$

(a) A surface in $\mathrm{ST}_{Ab}([6^2])$ with hyperelliptic involution $\alpha = (1,4)(2,3)(5,6)(7,12)(8,11)(9,10)$.

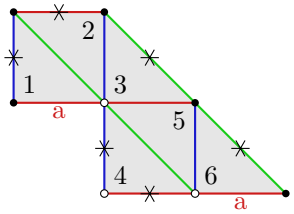

$\tau_R = (1,6)(2)(3,5)$
$\tau_G = (1,2)(3)(4,5)(6)$
$\tau_B = (1)(2,3)(4)(5,6)$

(b) The quotient of Figure 22a in $\mathrm{ST}_{quad}([3^2], 6)$.

Figure 22: A hyperelliptic square-tiled surface in $\mathrm{ST}_{Ab}([6^2])$ not in $\mathrm{ST}^{hyp}_{Ab}([6^2])$: the quotient belongs to $\mathrm{ST}_{quad}([3^2], 6)$.

Lemma 5.1. *For $g \geqslant 2$ and $\mu_2 \geqslant 0$, the quotient by the hyperelliptic involution induces the bijections*

$$\mathrm{ST}^{hyp}_{Ab}([2^{\mu_2}, 4g-2]) \to \bigcup_{\substack{k'+\mu'_1=2g+1 \\ \mu'_1+2\mu'_2=\mu_2}} \mathrm{ST}_{quad}([1^{\mu'_1}, 2^{\mu'_2}, 2g-1], k'). \tag{5}$$

and

$$\mathrm{ST}^{hyp}_{Ab}([2^{\mu_2}, (2g)^2]) \to \bigcup_{\substack{k'+\mu'_1=2g+2 \\ \mu'_1+2\mu'_2=\mu_2}} \mathrm{ST}_{quad}([1^{\mu'_1}, 2^{\mu'_2}, 2g], k'). \tag{6}$$

Proof. In the first case, the hyperelliptic involution preserves the singularity of degree $4g-2$. The image of this singularity in the quotient by the hyperelliptic involution is a singularity of degree $2g-1$. By Euler's characteristic computation, one obtains that $k' + \mu'_1 = 2g+1$.

In the second case, by definition, the hyperelliptic involution exchanges the two singularities of degree $2g$. The image of this pair of singularities in the quotient by the hyperelliptic involution is a singularity of degree $2g$. Again, by Euler's characteristic computation, one obtains that $k' + \mu'_1 = 2g+2$.

This proves that the quotient by the hyperelliptic involution indeed belongs to the right hand sides of (5) and (6) respectively.

We now briefly explain why these maps are bijections. This follows from the standard construction that to any quadratic square-tiled surface, one can associate a unique Abelian

square-tiled surface and an involution such that the quotient gives back the quadratic differential. □

The following lemma is a consequence of a result of Kontsevich and Zorich [KZ03, Section 2.1]. Alternatively, a direct combinatorial proof follows immediately from Lemma 5.4, stated in the next subsection after defining half cylinder shears.

Lemma 5.2. *Let $\mu = [2^{\mu_2}, 4g-2]$ or $\mu = [2^{\mu_2}, (2g)^2]$ for some $g \geqslant 2$ and $\mu_2 \geqslant 0$. Then $\mathrm{ST}^{hyp}_{Ab}(\mu)$ is preserved by cylinder shears.*

Remark 5.3. Let us mention that for quadratic square-tiled surfaces, there also exist hyperelliptic connected components, see [Lan08]. They correspond exactly to quadratic square-tiled surfaces in genus $g \geqslant 1$ that are hyperelliptic and whose quotient belongs to $\mathrm{ST}_{quad}(1^{\mu_1}, 2^{\mu_2}, a, b)$ where $a, b \geqslant 2$. That is, instead of having a single singularity $d \geqslant 3$ as in Lemma 5.1 on the sphere, there are two.

However, we were not able to apply the techniques we develop in this article in order to show the connectedness of $\mathrm{ST}^{hyp}_{quad}(\mu)$.

5.2 Half cylinder shears

At first glance, Lemma 5.1 and Conjecture 1.4 seem in contradiction. Namely, from (5), the quotient by the hyperelliptic involution maps the subset of square-tiled surfaces $\mathrm{ST}^{hyp}_{Ab}([2^{\mu_2}, 4g-2])$ to a disjoint union of $\mathrm{ST}_{quad}([1^{\mu'_1}, 2^{\mu'_2}, 2g-1], k')$. And Conjecture 1.4 asserts that the left side of (5) is connected under cylinder shears, while the right side is obviously not by Lemma 2.2. The reason is that if τ is a square-tiled surface in $\mathrm{ST}^{hyp}_{Ab}([2^{\mu_2}, 4g-2])$ and τ' its quotient by the hyperelliptic involution then a cylinder shear in τ does not necessarily correspond to a cylinder shear in τ'. One sometimes obtains what we call a *half cylinder shear* that modifies the profile and which we study now.

Let τ be a square-tiled surface and c a $\{G, B\}$-cycle that separates the square-tiled surface such that one of the connected components of the complement of c contains only hexagons, 1-faces and red half-edges. In more a combinatorial way, let $c = c_1 \sqcup c_2$ the decomposition into two $\tau_B \circ \tau_G$-orbits. We ask that c_1 is stable under τ_R and that the faces bounded by c together with the red edges with ends in c_1 are only hexagons and either two half-edges or two 1-faces. The horizontal *half cylinder shear* along c is obtained by changing τ_R along c_1 as follows (see also Figure 23)

$$\tau'_R(i) = \begin{cases} \tau_G \circ \tau_B \circ \tau_R(i) & \text{if } i \in c_1 \\ \tau_R(i) & \text{otherwise.} \end{cases}$$

We similarly define vertical half cylinder shears on $\{R, G\}$-cycles.

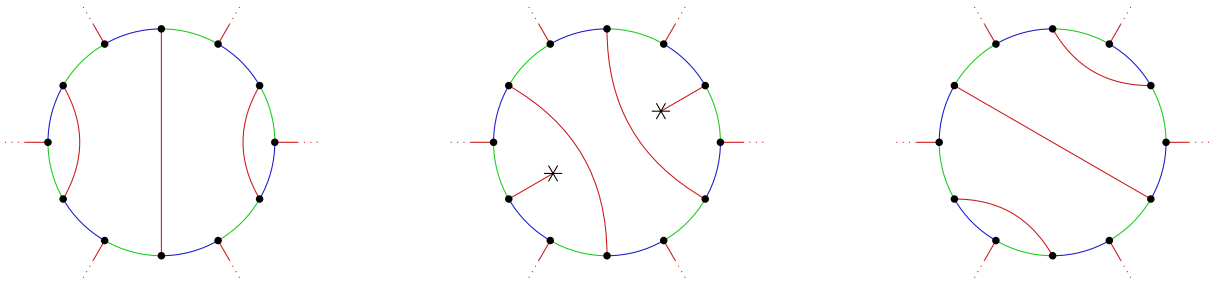

Figure 23: A cylinder shear as the composition of two half cylinder shears.

Similarly to the case of the cylinder shears, half cylinder shears induce a natural bijection on the vertices of $S^*(\tau)$, that we will not define here.

Lemma 5.4. *Let τ be a square-tiled surface of genus $g \geqslant 2$ in either $\mathrm{ST}^{hyp}_{Ab}([2^{\mu_2}, 4g-2])$ or $\mathrm{ST}^{hyp}_{Ab}([2^{\mu_2}, (2g)^2])$. Let τ' be its quotient by the hyperelliptic involution. Let c be a $\{G, B\}$-cycle in τ and c' its image in τ'.*

If c' belongs to a horizontal cylinder bounded by a $\{G, B\}$-path c'' (equivalently if the height h in the edge decoration (w, h) of the weighted stable graph $\Gamma(\tau')$ is a half integer) then the quotient of $\mathrm{Shear}_{c,B,G}(\tau)$ by the hyperelliptic involution is isomorphic to $\mathrm{Shear}_{c'',B,G}(\tau')$.

If c' belongs to a horizontal cylinder bounded by a $\{G, B\}$-cycle c'' isolating a component of $S^*(\tau')$ made only of hexagons and either red half-edges or 1-faces, then the quotient by the hyperelliptic involution of $\mathrm{Shear}_{c,B,G}(\tau)$ is isomorphic to the horizontal half cylinder shear along c'' in τ'.

Proof. We only sketch the proof, which is straightforward.

Each cylinder of $S(\tau)$ is preserved by the hyperelliptic involution. The first case corresponds to the situation where the height of the cylinder containing the curve c has odd height. In that case, the circumference in the middle of the cylinder is mapped to a component of the critical graph that corresponds to a $\{G, B\}$-path in $S^*(\tau)$. Performing a cylinder shear in c is the same as performing a cylinder shear along that $\{G, B\}$-path.

In the second case, when the height is even, the circumference is mapped to a component of the critical graph made of red edges. In that case, the cylinder shear in c becomes a horizontal half cylinder shear in the quotient. □

The lower bound of Theorem 1.6 is a direct consequence of Lemma 5.4. Its proof is very similar to that of Proposition 3.4 for spherical profiles, by considering half cylinder shear on top of cylinder shears.

Proposition 5.5. *Let $\mu \in \{[2^{\mu_2}, (2g)^2], [2^{\mu_2}, 4g-2]\}$, with $g > 1$. Then there are square-tiled surfaces in $\mathrm{ST}^{hyp}_{Ab}(\mu)$ that are separated by $\Omega(g)$ cylinder shears.*

Proof. Let μ'_1 and μ'_2 such that $\mu'_1 + 2\mu'_2 = \mu_2$ and $\mu'_1 \leqslant 1$. Let $k' = 2g + 1 - \mu'_1$ if μ is of the form $[2^{\mu_2}, 4g-2]$ and $k' = 2g + 2 - \mu'_1$ otherwise. Note that (μ', k') is a spherical profile and that $k' \geqslant 2g$. By Theorem 3.1, there is a path-like square-tiled surface τ of profile (μ', k'), and by symmetry, there is also a square tiled-surface σ of profile (μ', k') that has a single vertical cylinder which furthermore is a path.

A shear can only change by at most two the number of half-edges coloured red in $S^*(\tau)$. Likewise, a half cylinder shear changes the number of red half-edges by at most two. Since τ and σ have respectively $k' - 2$ and at most two red half-edges. By Lemma 5.1 and Lemma 5.4, the corresponding square-tiled surfaces of $\mathrm{ST}^{hyp}_{Ab}(\mu)$ are separated by at least $g - 2$ shears, which concludes the proof. □

5.3 Connecting to a path-like configuration

We continue to work on spherical square-tiled surface. We now describe how to circumvent the restriction $\mu_1 \leqslant 1$ on the profile when connecting to a path-like configuration as in Section 3 or when connecting two path-like configurations as in Section 4. The procedure uses the half cylinder shears introduced just before.

The analogue of Lemma 3.5 we prove in that context is the following.

Lemma 5.6. *Let τ be a spherical square-tiled surface with profile $([1^{\mu_1}, 2^{\mu_2}, d], k)$ where $d \geqslant 3$. Then τ can be connected with a sequence of $O(k + \mu_1)$ powers of cylinder shears and $O(\mu_1)$ half cylinder shears to a path-like square-tiled surface.*

Proof. Let τ be a spherical square-tiled surface with profile $([1^{\mu_1}, 2^{\mu_2}, d], k)$. The weighted stable tree $\Gamma(\tau)$ is a star whose center is the unique vertex v_0 whose decoration μ^{v_0} contains the element d of the profile. The other vertices, that necessarily are leaves, have decorations either equal to $([2^m], 2)$, or $([1, 2^m], 1)$ or $([1^2, 2^m], 0)$ where $m \geqslant 0$. For each leaf with decoration $([1^2, 2^m], 0)$, we use a half cylinder shear to turn it in to a leaf with decoration $([2^{m+1}], 2)$. We obtain a square-tiled surface satisfying the assumptions of Lemma 3.8 on which there hence exists a fusion path. Performing a vertical cylinder shear on that fusion path reduces the degree of the special vertex v_0 in $\Gamma(\tau)$.

Now it remains to treat the case when the degree of v_0 is one. In that case, $\Gamma(\tau)$ has a single other vertex v_1 with decoration either $([2^m], 2)$, or $([1, 2^m], 1)$ or $([1^2, 2^m], 0)$ with $m \geqslant 0$. If v_0 is such that its decoration satisfies $k^{(v_0)} > 0$, then up to performing a horizontal half cylinder shear in v_1, one can also use Lemma 3.8 to find a fusion path. We now further assume that $k(v_0) = 0$. Up to a horizontal half cylinder shear, one can assume that $\mu_1^{(v_1)} > 0$. It is easy to see that there exists a $\{R, G\}$-cycle c that "connects" a 1-face in v_0 to a 1-face in v_1 in the following sense: c crosses every $\{G, B\}$-components exactly twice and one of the connected component of the complement of c consists only of hexagons and two 1-faces. Performing a vertical half cylinder shear in c results in a path like configuration (see Figure 24). □

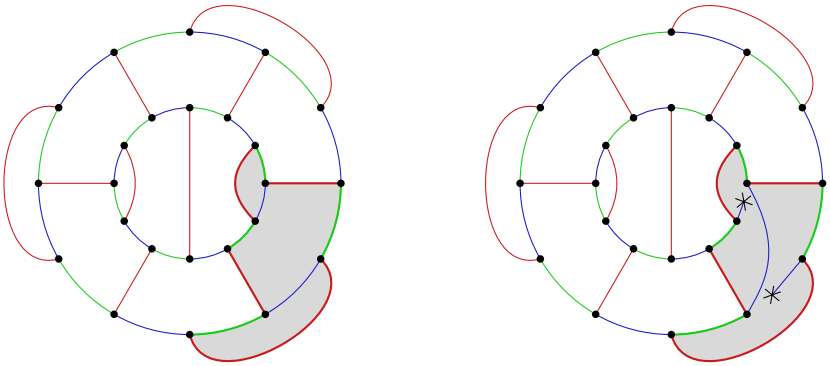

Figure 24: A $\{R, G\}$-cycle in $S^*(\tau)$ as used in the proof of Lemma 5.6. The shaded region is made of two 1-faces and one 2-face (or hexagon).

5.4 Reducing to the spherical case: proof of Theorem 1.6

We focus on the upper bound of Theorem 1.6, as the lower bound was proven by Proposition 5.5.

Proof of Theorem 1.6. Let us consider a square-tiled surface in either $\mathrm{ST}_{Ab}^{hyp}([2^{\mu_2}, (2g)^2])$ or $\mathrm{ST}_{Ab}^{hyp}([2^{\mu_2}, 4g-2])$ for some $\mu_2 \geqslant 0$. By Lemma 5.1, its quotient by the hyperelliptic involution belongs to respectively either a stratum $\mathrm{ST}_{quad}([1^{\mu_1'}, 2^{\mu_2'}, 2g-1], k')$ or $\mathrm{ST}_{quad}([1^{\mu_1'}, 2^{\mu_2'}, 2g], k')$ for some $\mu_1', \mu_2', k' \geqslant 0$. By Lemma 5.4, the cylinder shears in τ correspond to cylinder shears or half cylinder shears in the quotients. Hence, it is enough to connect $\bigcup_{\substack{k'+\mu_1'=2g+1 \\ \mu_1'+2\mu_2'=\mu_2}} \mathrm{ST}_{quad}([1^{\mu_1'}, 2^{\mu_2'},$

$2g-1], k')$ or $\bigcup_{\substack{k'+\mu_1'=2g+2\\ \mu_1'+2\mu_2'=\mu_2}} \mathrm{ST}_{quad}([1^{\mu_1'}, 2^{\mu_2'}, 2g], k')$ using both cylinder shears and half cylinder shears.

By Theorem 1.7 we know that cylinder shears are enough to connect the spherical strata when $\mu_1' \leqslant 1$. Let us first note that the parity of μ_1' is fixed by the profile (μ, k) by Lemma 2.1. Hence, depending on (μ, k) only one of the quotient stratum with $\mu_1' \leqslant 1$ is non-empty. What remains to do is to connect all spherical square-tiled surface to these base cases.

To do so, we first apply Lemma 5.6 that allows us to reach a path-like configuration $S^*(\tau)$.

Next, we explain how to remove pairs of 1-faces in $S^*(\tau)$ until there remains at most one of them (the corresponding sequence is illustrated by an example in Figure 25). Let A and B be two 1-faces of $S^*(\tau)$ (see Figure 25a). Perform in τ a power of the horizontal shear on the unique $\{G, B\}$-path until A and B share a blue edge e (see Figure 25b). Let f be the red edge in the boundary of A. Perform a vertical half cylinder shear on the $\{R, G\}$-cycle bounding $A \cup B$, this replaces e by two blue half-edges and thus cuts the $\{G, B\}$-path in two $\{G, B\}$-paths P_1 and P_2. This also changes the profile by trading two 1-faces for two half-edges and a hexagon (see Figure 25c). Perform a horizontal cylinder shear on P_1 and P_2 such that each of them has a extremity incident to f and a green half-edge (see Figure 25d). Perform a vertical cylinder shear on f and the incident green half-edges to obtain again a single $\{G, B\}$-path.

The resulting square-tiled surface is path-like and has two fewer 1-faces. By repeating this procedure inductively, one obtains a spherical path-like square-tiled surface τ' with at most one 1-face. In other words, the profile (μ', k') of τ' is spherical and has $\mu_1' \leqslant 1$. We reduced the general case to the two known base cases of Theorem 1.7 in $O(k + \mu_1)$ powers of cylinder shears and half cylinder shears. This concludes the proof of the theorem. □

6 Discussion

6.1 Equivalence via cylinder shears

The first open problem we consider is naturally Conjecture 1.4 in full generality. In this article, we confirmed Conjecture 1.4 in two special cases. First, in the Abelian hyperelliptic components (see Theorem 1.6). Second, on the sphere (see Theorem 1.7), in all strata when authorizing half-shears, but only in the strata such that $\mu_1 \leqslant 1$ and $(\mu, k) \neq ([1, 2^*, 3], 4)$ when restricting to regular shears. This suggest several milestones towards proving Conjecture 1.4, that isolate different points of failure of our proof. We present them ranked by increasing (supposed) difficulty:

The first question is whether the quadratic hyperelliptic components are also connected by cylinder shears. Our method to connect to a path-like configuration is specific to $\mu_1 \leqslant 1$ when using only cylinder shears, and to the strata with $\sum_{i \geqslant 3} \mu_i \leqslant 1$ when authorizing half-shears, which does not cover quadratic hyperelliptic components.

Finally, we conjecture the following, which is a special case of Conjecture 1.4 and generalises Theorem 1.7 to spherical profiles with $\mu_1 \geqslant 2$:

Conjecture 6.1. *Let (μ, k) be a spherical profile. The set of square-tiled surfaces $\mathrm{ST}(\mu, k)$ is connected by cylinder shears.*

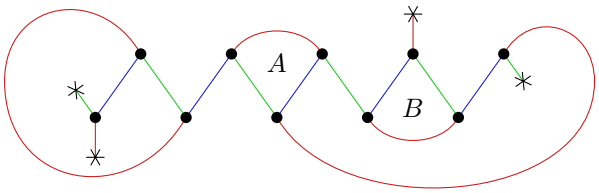

(a) Starting configuration.

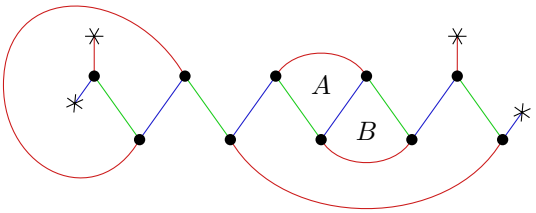

(b) After a power of a horizontal shear the two 1-faces A and B are adjacent and separated by a blue edge e.

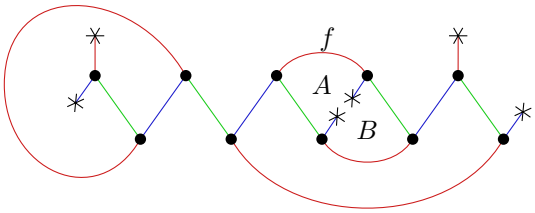

(c) After a vertical half cylinder shear, e is replaced by two blue half-edges. This impacts the profile.

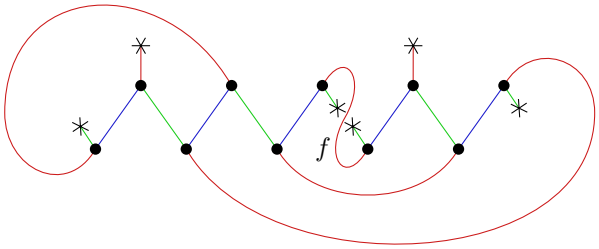

(d) After two horizontal shears, a red edge f originally on the boundary of A is now adjacent to the extremities of both $\{G, B\}$-paths.

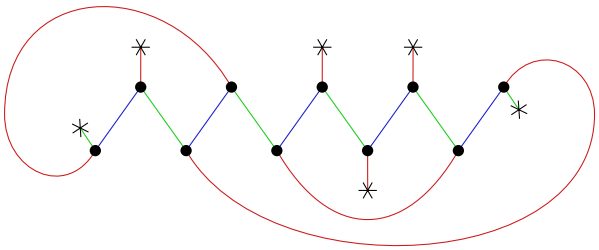

(e) Final configuration, obtained by performing the vertical shear containing f.

Figure 25: Removing pairs of 1-faces in the path-like configuration.

6.2 Further remarks

There is an action of $\mathrm{SL}_2(\mathbb{Z})$ on square-tiled surfaces that is a natural restriction of an $\mathrm{SL}_2(\mathbb{R})$-action on Abelian and quadratic differentials. This action can easily be rephrased in terms of cylinder shears: the action of $\begin{pmatrix} 1 & 1 \\ 0 & 1 \end{pmatrix}$ and $\begin{pmatrix} 1 & 0 \\ 1 & 1 \end{pmatrix}$ corresponds to simultaneous cylinder shears in respectively all horizontal and vertical cylinders. Since these two matrices generate $\mathrm{SL}_2(\mathbb{Z})$, connected components of the $\mathrm{SL}_2(\mathbb{Z})$ reconfiguration graph are finer than for cylinder shears. The classification of these connected components, even conjecturally, is open in general. Beyond the elementary case of the stratum $\mathcal{H}(\emptyset)$ on the torus, only partial results are known in genus 2 and in the so-called Prym loci, see [McM05, HL06, LN20, Dur].

Beyond its interest as a delicate reconfiguration problem, it would be interesting to investigate more the geometric significance of cylinder shears on square-tiled surfaces. It is

well-known that the cardinality of $\mathrm{ST}(\mu, k)$ is related to the so-called Masur–Veech measure of strata of Abelian and quadratic differentials [Zor02]. Though the link between the geometry (e.g. the diameter) of the cylinder shear reconfiguration graph and connected components of strata remains to explore. In particular, it seems plausible that the mixing rate of the cylinder shear dynamics is related to the spectral gap of the $\mathrm{SL}_2(\mathbb{R})$-action on the connected components of strata of Abelian and quadratic strata established in [AGY06, AG13].

Finally, cylinders shears on square-tiled surfaces present surprising similarities with a reconfiguration operation on the colourings of a graph. Two reconfiguration operations on colourings have been considered: single vertex recolouring that consists in changing the colour of a single vertex and Kempe changes that are more complex but are crucial in the proof of the celebrated Four Colour Theorem. Like Kempe changes, cylinder shears can affect an arbitrarily large part of the configuration. This non-locality complicates the analysis of the reconfiguration graph, in particular, most of the arguments to prove rapid mixing of the associated Markov chains do not seem to apply to such chains. As we observed at the end of Subsection 2.2, there are deeper connections between cylinder shears and Kempe changes on edge colourings, which suggest that developments of methods to analyse the mixing of one of these chains may transfer to the other.

References

[AG13] Artur Avila and Sébastien Gouëzel. Small eigenvalues of the Laplacian for algebraic measures in moduli space, and mixing properties of the Teichmüller flow. *Ann. Math. (2)*, 178(2):385–442, 2013.

[AGY06] Artur Avila, Sébastien Gouëzel, and Jean-Christophe Yoccoz. Exponential mixing for the Teichmüller flow. *Publ. Math., Inst. Hautes Étud. Sci.*, 104:143–211, 2006.

[Ald94] David Aldous. Triangulating the circle, at random. *Am. Math. Mon.*, 101(3):223–233, 1994.

[AM24] Jayadev S. Athreya and Howard Masur. *Translation surfaces (to appear).* Providence, RI: American Mathematical Society (AMS), 2024.

[BLdM+22] Maike Buchin, Anna Lubiw, Arnaud de Mesmay, Saul Schleimer, and Florestan Brunck. Computation and Reconfiguration in Low-Dimensional Topological Spaces (Dagstuhl Seminar 22062). *Dagstuhl Reports*, 12(2):17–66, 2022.

[Bud17] Thomas Budzinski. On the mixing time of the flip walk on triangulations of the sphere. *C. R., Math., Acad. Sci. Paris*, 355(4):464–471, 2017.

[CFZ11] Julien Cassaigne, Sébastien Ferenczi, and Luca Q. Zamboni. Combinatorial trees arising in the study of interval exchange transformations. *Eur. J. Comb.*, 32(8):1428–1444, 2011.

[CHK+18] Jean Cardinal, Michael Hoffmann, Vincent Kusters, Csaba D. Tóth, and Manuel Wettstein. Arc diagrams, flip distances, and Hamiltonian triangulations. *Comput. Geom.*, 68:206–225, 2018.

[CS20] Alessandra Caraceni and Alexandre Stauffer. Polynomial mixing time of edge flips on quadrangulations. *Probab. Theory Relat. Fields*, 176(1-2):35–76, 2020.

[DGZ+20] Vincent Delecroix, Élise Goujard, Peter Zograf, Anton Zorich, and Engel. Contribution of one-cylinder square-tiled surfaces to Masur-Veech volumes. In *Some aspects of the theory of dynamical systems: a tribute to Jean-Christophe Yoccoz. Volume I*, pages 223–274. Paris: Société Mathématique de France (SMF), 2020.

[DGZZ20] Vincent Delecroix, Elise Goujard, Peter Zograf, and Anton Zorich. Enumeration of meanders and Masur–Veech volumes. In *Forum of Mathematics, Pi*, volume 8, page e4. Cambridge University Press, 2020.

[DGZZ21] Vincent Delecroix, Élise Goujard, Peter Zograf, and Anton Zorich. Masur-Veech volumes, frequencies of simple closed geodesics, and intersection numbers of moduli spaces of curves. *Duke Math. J.*, 170(12):2633–2718, 2021.

[DP19] Valentina Disarlo and Hugo Parlier. The geometry of flip graphs and mapping class groups. *Trans. Am. Math. Soc.*, 372(6):3809–3844, 2019.

[Dur] Eduard Duryev. Teichmüller curves in genus two: Square-tiled surfaces and modular curve. arXiv:1905.09312 [math.GT].

[EF23] David Eppstein and Daniel Frishberg. Improved mixing for the convex polygon triangulation flip walk, 2023.

[FM11] Benson Farb and Dan Margalit. *A primer on mapping class groups*, volume 49 of *Princeton Math. Ser.* Princeton, NJ: Princeton University Press, 2011.

[Fra17] Fabrizio Frati. A lower bound on the diameter of the flip graph. *Electron. J. Comb.*, 24(1):research paper p1.43, 6, 2017.

[FZ10] Sébastien Ferenczi and Luca Q. Zamboni. Structure of K-interval exchange transformations: induction, trajectories, and distance theorems. *J. Anal. Math.*, 112:289–328, 2010.

[HL06] Pascal Hubert and Samuel Lelièvre. Prime arithmetic Teichmüller discs in $\mathcal{H}(2)$. *Isr. J. Math.*, 151:281–321, 2006.

[KZ03] Maxim Kontsevich and Anton Zorich. Connected components of the moduli spaces of Abelian differentials with prescribed singularities. *Invent. Math.*, 153(3):631–678, 2003.

[Lan08] Erwan Lanneau. Connected components of the strata of the moduli spaces of quadratic differentials. *Ann. Sci. Éc. Norm. Supér. (4)*, 41(1):1–56, 2008.

[LN20] Erwan Lanneau and Duc-Manh Nguyen. Weierstrass Prym eigenforms in genus four. *J. Inst. Math. Jussieu*, 19(6):2045–2085, 2020.

[LP17] David A Levin and Yuval Peres. *Markov chains and mixing times*, volume 107. American Mathematical Soc., 2017.

[McM05] Curtis T. McMullen. Teichmüller curves in genus two: Discriminant and spin. *Math. Ann.*, 333(1):87–130, 2005.

[MN19] CM Mynhardt and S Nasserasr. Reconfiguration of colourings and dominating sets in graphs. In *50 Years of Combinatorics, Graph Theory, and Computing*, pages 171–191. Chapman and Hall/CRC, 2019.

[Mos88] Lee Mosher. Tiling the projective foliation space of a punctured surface. *Trans. Am. Math. Soc.*, 306(1):1–70, 1988.

[MRS99] Michael Molloy, Bruce Reed, and William Steiger. On the mixing rate of the triangulation walk. In *Randomization methods in algorithm design. DIMACS workshop, Princeton Univ., NJ, USA, December 12–14, 1997*, pages 179–190. Providence, RI: AMS, American Mathematical Society, 1999.

[Nis18] Naomi Nishimura. Introduction to reconfiguration. *Algorithms*, 11(4):52, 2018.

[Pou14] Lionel Pournin. The diameter of associahedra. *Adv. Math.*, 259:13–42, 2014.

[PP17] Hugo Parlier and Lionel Pournin. Flip-graph moduli spaces of filling surfaces. *J. Eur. Math. Soc. (JEMS)*, 19(9):2697–2737, 2017.

[PP18a] Hugo Parlier and Lionel Pournin. Modular flip-graphs of one-holed surfaces. *Eur. J. Comb.*, 67:158–173, 2018.

[PP18b] Hugo Parlier and Lionel Pournin. Once punctured disks, non-convex polygons, and pointihedra. *Ann. Comb.*, 22(3):619–640, 2018.

[STT88] Daniel D. Sleator, Robert E. Tarjan, and William P. Thurston. Rotation distance, triangulations, and hyperbolic geometry. *J. Am. Math. Soc.*, 1(3):647–681, 1988.

[STT92] Daniel D. Sleator, Robert E. Tarjan, and William P. Thurston. Short encodings of evolving structures. *SIAM J. Discrete Math.*, 5(3):428–450, 1992.

[vdH13] Jan van den Heuvel. The complexity of change. *Surveys in combinatorics*, 409(2013):127–160, 2013.

[Zor02] Anton Zorich. Square tiled surfaces and Teichmüller volumes of the moduli spaces of Abelian differentials. In *Rigidity in dynamics and geometry. Contributions from the programme Ergodic theory, geometric rigidity and number theory, Isaac Newton Institute for the Mathematical Sciences, Cambridge, UK, January 5–July 7, 2000*, pages 459–471. Berlin: Springer, 2002.

[Zor06] Anton Zorich. Flat surfaces. In *Frontiers in number theory, physics, and geometry I. On random matrices, zeta functions, and dynamical systems. Papers from the meeting, Les Houches, France, March 9–21, 2003*, pages 437–583. Berlin: Springer, 2nd printing edition, 2006.

[Zor08] Anton Zorich. Explicit Jenkins-Strebel representatives of all strata of Abelian and quadratic differentials. *J. Mod. Dyn.*, 2(1):139–185, 2008.